JOURNAL OF VIROLOGY, Aug. 2005, p. 9954–9969 Vol. 79, No. 15
0022-538X/05/$08.00+0 doi:10.1128/JVI.79.15.9954–9969.2005

Soluble Mimetics of Human Immunodeficiency Virus Type 1 Viral Spikes Produced by Replacement of the Native Trimerization Domain with a Heterologous Trimerization Motif: Characterization and Ligand Binding Analysis

Marie Pancera,[1] Jacob Lebowitz,[2] Arne Schön,[3] Ping Zhu,[4] Ernesto Freire,[3] Peter D. Kwong,[1] Kenneth H. Roux,[4] Joseph Sodroski,[5] and Richard Wyatt[1]*

Vaccine Research Center, NIH, Bethesda, Maryland 20892[1]; Division of Bioengineering and Physical Science, NIH, Bethesda, Maryland 20892[2]; Department of Biology, The Johns Hopkins University, Baltimore, Maryland 21218[3]; Department of Biological Science and Institute of Molecular Biophysics, Florida State University, Tallahassee, Florida 32306[4]; and Dana Farber Cancer Institute, Boston, Masssachusetts 02115[5]

Received 9 February 2005/Accepted 13 April 2005

The human immunodeficiency virus type 1 (HIV-1) exterior envelope glycoprotein, gp120, mediates binding to the viral receptors and, along with the transmembrane glycoprotein gp41, is a major target for neutralizing antibodies. We asked whether replacing the gp41 fusion/trimerization domain with a stable trimerization motif might lead to a more stable gp120 trimer that would be amenable to structural and immunologic analysis. To obtain stable gp120 trimers, a heterologous trimerization motif, GCN4, was appended to the C terminus of YU2gp120. Biochemical analysis indicated that the gp120-GCN4 trimers were superior to gp140 molecules in their initial homogeneity, and trilobed structures were observable by electron microscopy. Biophysical analysis of gp120-GCN4 trimers by isothermal titration calorimetry (ITC) and ultracentrifugation analyses indicated that most likely two molecules of soluble CD4 could bind to one gp120-GCN4 trimer. To further examine restricted CD4 stoichiometric binding to the gp120-GCN4 trimers, we generated a low-affinity CD4 binding trimer by introducing a D457V change in the CD4 binding site of each gp120 monomeric subunit. The mutant trimers could definitively bind only one soluble CD4 molecule, as determined by ITC and sedimentation equilibrium centrifugation. These data indicate that there are weak interactions between the gp120 monomeric subunits of the GCN4-stabilized trimers that can be detected by low-affinity ligand sensing. By similar analysis, we also determined that removal of the variable loops V1, V2, and V3 in the context of the gp120-GCN4 proteins allowed the binding of three CD4 molecules per trimer. Interestingly, both the gp120-GCN4 variants displayed a restricted stoichiometry for the CD4-induced antibody 17b of one antibody molecule binding per trimer. This restriction was not evident upon removal of the variable loops V1 and V2 loops, consistent with conformational constraints in the wild-type gp120 trimers and similar to those inherent in the functional Env spike. Thus, the gp120-GCN4 trimers demonstrate several properties that are consistent with some of those anticipated for gp120 in the context of the viral spike.

The human immunodeficiency virus type 1 (HIV-1) envelope glycoproteins, gp120 and gp41, form a specialized type I viral membrane fusion complex that mediates viral entry (18). The gp120 constitutes the receptor binding domain that interacts with the viral receptors CD4 and CCR5/CXCR4 (17, 21, 22). The HIV-1 gp41 contains the trimerization domain and mediates virus-to-target cell membrane fusion (24). The gp41 glycoprotein comprises an ectodomain, which contains two heptad repeats (heptad repeats 1 [HR1] and 2 [HR2]) that provide the machinery for membrane fusion, a transmembrane anchor and cytoplamic tail (Fig. 1A) (61). A likely model of the metastable viral envelope spike is that elements of gp120 maintain gp41 in a prefusogenic conformation. These interactions prevent the large interactive surfaces of HR1 and HR2 from collapsing into the low-free-energy six-helix bundle conformation that drives the membrane fusion process and has been resolved by crystallography (16, 62).

Presumably due to its exposed location at the surface of the human immunodeficiency virus, the glycoprotein spike is the major target for neutralizing antibodies. Attempts to elicit broadly neutralizing antibodies using both monomeric gp120 (1–4, 19, 40, 65), peptides from gp41 (41, 49), or soluble gp140 mimics of the envelope spike (23, 58) have been met with limited success. It is likely that knowledge of the fine structure of the envelope glycoproteins as they exist on the surface will enhance our ability to better design immunogens capable of more efficiently eliciting neutralizing antibodies. In this regard, we have attempted to produce soluble, stable trimers containing the entire HIV-1 exterior envelope glycoprotein, gp120, and to potentially define the functional properties inherent in the gp120 subunit of the spike.

* Corresponding author. Mailing address: Structural Virology Section, Vaccine Research Center/NIH, 40 Convent Dr., Bethesda, MD 20892. Phone: (301) 594-8690. Fax: (301) 480-2658. E-mail: richardwyatt@nih.gov.

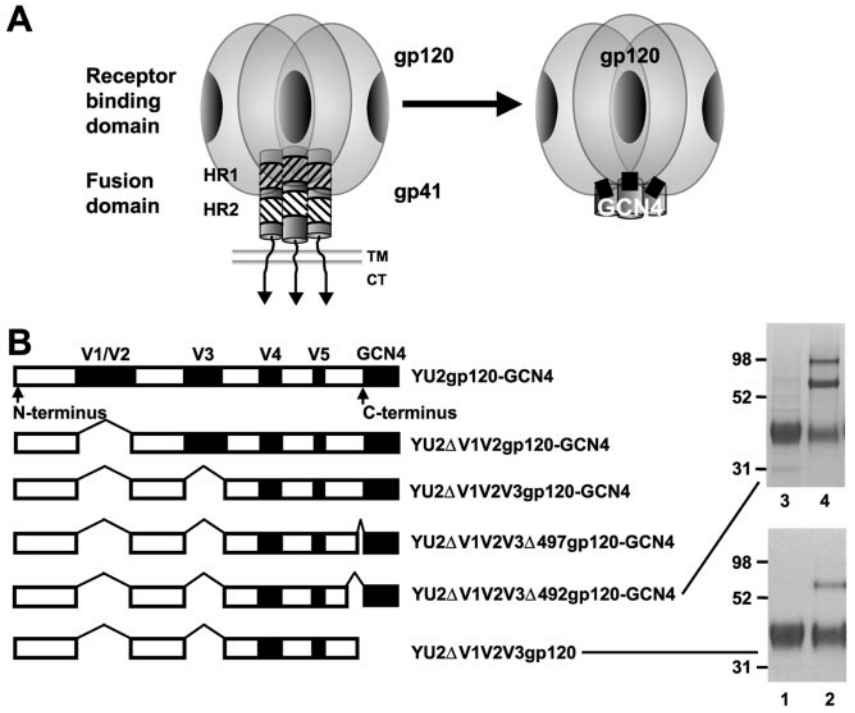

FIG. 1. (A, left) Schematic representation of the HIV-1 viral type 1 membrane fusion protein comprising (i) the gp120 receptor binding domain and (ii) the gp41 oligomerization and fusion domains, the transmembrane anchor, and the cytoplasmic tail. The heptad repeats of gp41 are indicated by crosshatching and labeled HR1 and HR2. (A, right) GCN4 trimerization coiled coil, replacing gp41, was appended at the C terminus of the gp120. Gray ovals, CD4 binding site region; ■, cleavage site mutated to be cleavage defective. (B.) Variant trimeric gp120 glycoproteins were generated, with deletion of the variable loops and of the C terminus (at aa 492 and 497) as schematically diagrammed. An SDS gel of the ΔV1V2V3gp120 and ΔV1V2V3Δ492gp120-GCN4 glycoproteins is shown. Lane 1, ΔV1V2V3gp120 reduced; lane 2, ΔV1V2V3gp120 nonreduced; lane 3, ΔV1V2V3Δ492gp120-GCN4 reduced; lane 4, YU2ΔV1V2V3Δ492gp120-GCN4 nonreduced.

Overwhelming evidence indicates that the native Env spike is a trimer of gp120-gp41 heterodimers (13, 15, 28, 62, 67, 74). However, the fine structure of the spike has not been elucidated at the atomic level of resolution. Nor have the current attempts to mimic the spike by various forms of soluble gp140 molecules (gp120 plus the gp41 ectodomain) been successful at eliciting antibodies of great breadth, although such molecules are an antigenic and immunogenic advance over monomeric gp120 (25). In general, gp140 molecules are not homogenous oligomers, although in at least one case, relatively homogeneous gp140 trimers have been reported (73). In most cases, oligomeric heterogeneity is observed, but a major fraction of the gp140 proteins can be purified to a high level of homogeneity consistent with a native trimeric architecture. This is true for gp140 molecules harboring heterologous trimerization domains such as GCN4 or foldon that we have characterized previously (54, 69–72), as well as most soluble oligomers not containing heterologous sequences (54, 57, 58). Very recently, it has been shown that chimeric constructs of HIV-1 gp120 and SIV gp41 generate stable gp140 trimers (14).

Therefore, guided in part by influenza hemagglutinin biochemical and structural information (6, 8, 64), we attempted to produce soluble gp120 trimers that would mimic the native orientation of gp120 in the envelope spike. The strategy that we followed was to replace the native gp41 oligomerization and fusion domains by a heterologous trimerization motif, a modified coiled-coil GCN4 (26, 46) at the gp120 C terminus, guided by previous studies demonstrating that the gp120 C terminus interacts with gp41 (10, 27, 70).

We then produced such molecules in quantities sufficient to characterize their oligomeric nature and by biochemical, biophysical, and antigenic analyses, to assess how closely they would display properties of previously characterized gp140 molecules, as well as properties associated with the bona fide native spike structure. Many of the properties of gp120 are known to differ dramatically between the monomeric and the trimeric gp120/gp41 state in the viral spike (7, 30, 44, 55), especially in terms of conformational constraints expected to exist on the functional spike. A gp120 trimer might enable us to see which of these properties relates solely to the trimerization of gp120 and which results from specific interactions with gp41. Following biochemical and morphological analyses, we studied the interactions of the primary receptor, CD4, the broadly neutralizing antibody, immunoglobulin G (IgG) b12 and the CD4-induced antibody 17b with selected trimers by isothermal titration calorimetry (ITC). Because the data suggested there was a possible restriction of CD4 binding to the trimers (on average, two CD4 molecules could bind the gp120-GCN4 trimers) and because a previous study of SIV gp140 trimers had observed a restricted stoichiometry in association with lower CD4 affinity (29), we also produced a mutant gp120 trimer possessing lower CD4 affinity and examined the thermodynamic properties of these variant trimers. To enhance the potential of the gp120-GCN4 molecules to crystallize, we also

deleted the variable loops and appended the heterologous trimerization motif at different positions nearby to the natural C-terminal cleavage site. The V1-V2-V3 loop-deleted trimers were also analyzed similarly to the wild-type (WT) trimer and we found that three molecules of CD4 or IgGb12 can bind to the loop-deleted trimer by ITC and sedimentation velocity. We also studied the interactions of the gp120-GCN4 trimers with the CD4-induced antibody 17b. The 17b IgG displays a restricted stoichiometry of binding only one antibody molecule per trimer; however, when the variable loops V1 and V2 are deleted, three molecules of 17b can bind to the trimer.

Here, we report our initial biochemical, biophysical, and antigenic analyses of WT and variant YU2gp120-GCN4 glycoproteins produced in *Drosophila* Schneider 2 (S2) insect cells. These analyses reveal some interesting properties of the proteins that suggest they possess intermonomeric subunit interactions relevant to the native spike structure. Moreover, this set of molecules may present a means of obtaining an initial high-resolution structure of the gp120 component of the viral spike.

MATERIALS AND METHODS

Construction of gp120 expression plasmids. The YU2gp120-GCN4 expression plasmids were derived from YU2gp140 (with or without GCN4) plasmid (kindly provided by Mike Farzan [70]) by deletion of the gp41 domain immediately following the cleavage defective site (SEKS) by the Quick Change Mutagenesis (QCM) reaction. A Gly-Gly linker replaced the gp41 domain. The hypervariable loops V1/V2 (amino acids [aa] 128 to 190) and/or V3 (aa 293 to 317) were deleted by QCM and replaced by a Gly-Ala-Gly linker to generate the gp120ΔV1V2-GCN4 and gp120ΔV1V2V3-GCN4 constructs (Fig. 1B). For the mutant proteins, the mutation was introduced at residue 457 (D457V) using QCM protocol, and the plasmids were sequenced. C-terminal deletions (aa 492 to 511 and aa 497 to 511) were accomplished by the same method to generate gp120ΔV1V2V3Δ492-GCN4 and gp120ΔV1V2V3Δ497-GCN4. The amino acid numbering is based on the prototypic HIV-1 HXBc2 strain according to current conventions (32). A YU2gp120 monomeric WT construct was used as a control protein for these studies.

The gp120-GCN4 coding sequences were amplified by PCR with primers containing 5′ BamH1 and 3′ Xba1 sites and were cloned into the insect expression vector pMT (20), using the compatible restriction sites BglII and NheI in pMT downstream and in frame with the tissue plasminogen activator leader (47). Thus, gp120 expression was placed under the control of the inducible metallothionein promoter in the pMT vector. All gp120-GCN4 open reading frames were confirmed by sequencing, and contiguous sequences were reconstructed using overlapping sequences in vector NTI.

Generation of stable *Drosophila* S2 cell lines. The S2 cells were seeded at 3×10^6 cells per well in a six-well tissue culture plate. The pMT gp120 expression constructs were cotransfected into S2 cells with the plasmid pcoHygro (ratio, 1:20) using FuGENE6 as per the manufacturer's instructions (Roche). The S2 cells were cultured in Insect-Xpress serum-free medium (Cambrex) at 25°C in room air incubators. Forty-eight hours after transfection, hygromycin B (Roche) was added to the cultures at a final concentration of 300 μg/ml. After 2 to 3 weeks of selection, the stable lines were then shaken at 80 rpm to enhance cell growth. Following growth to a density of $\sim 10^7$/ml in a volume of 20 ml, the cells were induced by the addition of $CuSO_4$ to the medium at a final concentration of 0.75 mM for 1 week. Protein expression was assessed by immunoprecipitation with several anti-gp120 antibodies and Coomassie gels. If the lines produced the anticipated protein, they were then expanded to a volume of 1 to 2 liters and induced with 0.75 mM of $CuSO_4$ for 1 week. The supernatant was then collected by spinning out the S2 cells and filtered through a 0.45-μm filter.

Purification of proteins by F105 affinity chromatography. The F105 affinity column was made by covalently coupling the F105 antibody (48) to protein A-Sepharose (Pierce). The filtered supernatant was then applied to the F105 affinity column to purify gp120 proteins. The column was washed twice with 10 times its volume of 0.5 M NaCl phosphate-buffered saline (PBS), and the protein was eluted using 3 M $MgCl_2$–20 mM Tris (pH 7.4) for the trimeric protein (GCN4 motif) or with 100 mM glycine, pH 2.8, and immediately neutralized to pH 7.4 with 1 M Tris base for the monomeric proteins. The trimeric proteins were dialyzed extensively against PBS to remove $MgCl_2$.

The optical density (OD) of the protein solution was read at 280 and 320 nm. Protein concentration was determined as follows: $C = [(OD_{280} - OD_{320}) \times \text{dilution}]/\text{extinction coefficient}$. The extinction coefficient (ε) was determined using protein analysis program in vector NTI. For initial analysis, sodium dodecyl sulfate-polyacrylamide gel electrophoresis (SDS-PAGE) was run under reducing and nonreducing conditions in MES (morpholineethanesulfonic acid) buffer (Invitrogen). The proteins were flash frozen in liquid nitrogen and stored at −80°C until further use.

Size exclusion chromatography (SEC). The affinity-purified proteins were submitted to further purification using a Superdex 200 16/26 column (Amersham Pharmacia) in PBS containing 0.35 M NaCl. The flow rate was set to 1 ml/min for the first 100 min and reduced to 0.5 ml/min until the end of the run, which allowed separation of the oligomeric states. The different fractions, as determined by OD_{280} adsorption peaks, were separated, collected, and concentrated. The proteins were flash frozen in liquid nitrogen and stored at −80°C until further use.

Blue native gels. The different column fractions obtained by gel filtration were run on blue native gels to confirm the oligomeric state of the gp120 glycoproteins. The running buffer was composed of 50 mM Tris HCl–50 mM MOPS (morpholinepropanesulfonic acid; pH 7.7) and was added to the outer chamber. The inner chamber contained the same running buffer with 10 mg of SERVA-G per 0.5 liter of buffer.

Novex gel system (Invitrogen) was used to run the gel: 10 μl of the 2× running sample buffer (100 mM Tris HCl, 100 mM MOPS, 40% glycerol, 0.1% Serva-G, pH 7.7) were added to 10 μl of the protein fraction and run overnight at 4°C at 30 mV. Standard molecular weight calibration markers (Amersham Pharmacia) were included in the analysis. Following electrophoresis, the gel was then stained using Coomassie and destained by normal procedures used for SDS-containing gels.

Light scattering, mass spectrometry, and analytical ultracentrifugation analyses. (i) Size exclusion chromatography with online multiangle light-scattering (SEC-MALS) measurements. Size exclusion chromatography with online detection of the resolved molecular weight components by Rayleigh light-scattering and absorbance measurements was used to characterize the purity of the respective gp120 preparations. In separate experiments, a 50-μl solution of either 1 mg/ml (gp120 trimer) or 1.5 mg/ml (gp120 monomer) was injected into a buffer-equilibrated (PBS with 0.35 M NaCl) TSK SW3000 SEC column (Tosoh Biosciences). The eluant from the SEC column, at a flow rate 0.2 ml/min, entered the UV detector (Waters 2487), followed by flow into the multiangle light-scattering detector (Wyatt Technology Dawn EOS). Wyatt Technology Astra software was used for data collection and analysis.

(ii) Matrix-assisted laser desorption ionization–time of flight mass spectrometry (MALDI-TOF MS). MALDI-TOF-MS analysis was performed for the molar mass determination of the gp120 monomer using an Applied Biosystems Voyager Elite DE-STR MALDI-TOF mass spectrometer (Framingham, MA). The instrument was operated in positive ion-linear mode at 25 kV accelerating voltage and a 750-ns ion extraction delay. Samples were applied to the MALDI sample plate using a "sandwich" method as follows. First, a 0.5-μl aliquot of matrix, a saturated solution of sinapinic acid in 1:1 acetonitrile and 0.1% trifluoroacetic acid, was applied to the plate and allowed to air dry. Then, a total of 5 μl of sample (applied 1 μl at a time and allowed to air dry in between applications) was applied over the dried matrix spot. Finally, an additional 0.5 μl of matrix was applied over the dried sample spot.

(iii) Sedimentation equilibrium measurements of the molar mass. In sedimentation equilibrium, the concentration distribution generally approaches an exponential; for a mixture of noninteracting ideal solutes, the measured signal as a function of radial position, $a(r)$, takes the following form:

$$a(r) = \sum_n c_{n.o}\varepsilon_n d \exp\left[\frac{M_n(1-\bar{\upsilon}_n\rho)\omega^2}{2RT}(r^2 - r_o^2)\right] + \delta \quad (1)$$

here the summation is over all species n. $c_{n.o}$ is the molar concentration of species n at a reference position r_o; M_n and $\bar{\upsilon}_n$ indicate the molar mass and partial specific volume of the species n, respectively; ε_n is the molar extinction coefficient; and d is the optical path length (usually 1.2 cm). δ is a baseline offset, which compensates for differences in nonsedimenting absorbing solutes between sample and reference compartments and small nonidealities in the cell assemblies (see reference 37 for a review of sedimentation equilibrium analysis). For a single component, the summation sign would be removed from equation 1. A mixture of components would yield an exponential that is the sum of the exponentials of the n components, and one could obtain

a weight average molar mass for this mixture. The ability to determine molar mass from equation 1 requires knowledge of the $\bar{\upsilon}$ of the macromolecule; for a glycoprotein, the best approach is the experimental determination of the weight fraction of the protein (w_p) and carbohydrate (w_c) portion of the molecule, respectively. MALDI-TOF MS analysis of the gp120 monomer gave a molar weight of 83,782 (molar weight of the protein portion from amino acid composition is 52,610) yielding a w_p of 0.628 and w_c of 0.372. For the gp120 trimer construct (molar weight of the protomer of the trimer is 56,403), we calculate weight fractions w_p of 0.644 and w_c of 0.356, assuming no differences in glycosylation between the monomer and trimer. The partial specific volume of a glycoprotein ($\bar{\upsilon}_{gp}$) is obtained from the relationship that $\bar{\upsilon}_{gp} = wp\bar{\upsilon}p + wc\bar{\upsilon}_c$, where $\bar{\upsilon}_p$ and $\bar{\upsilon}_c$ are the protein and carbohydrate partial specific volumes, respectively. The average molar weight of carbohydrate per glycosylation site is 1,417, based on 22 sites on one gp120 molecule. Since each site contains two *N*-acetylglucosamine residues, we obtain an average of 6.24 mannose residues per site and respective weight fractions of 0.286 and 0.714. The weighted sum of the partial specific volumes of *N*-acetylglucosamine (0.684 ml/g) and mannose residues (0.607 ml/g) gives a $\bar{\upsilon}_c$ of 0.629 ml/g (38). Using this $\bar{\upsilon}_c$ plus the corresponding protein weight fractions and $\bar{\upsilon}_p$ values for the monomer (0.725 ml/g) and the trimer (0.727 ml/g), we obtain $\bar{\upsilon}_{gp}$ values of 0.689 and 0.692 ml/g for the monomer and trimer gp120 constructs, respectively. The software program SEDNTERP (http://www.bbri-.org/RASMB/rasmb.html) developed by Hayes, Laue, and Philo was used to calculate $\bar{\upsilon}_p$ from the amino acid composition of the protein.

Sedimentation equilibrium measurements were made with an Optima XL-A/I analytical ultracentrifuge (Beckman-Coulter Instruments). Cells were loaded with 135 μl of the gp120 monomer or trimer at an A_{280} of 0.732 or 0.297, respectively, based on the extinction coefficient of the protein portion of each glycoprotein. The glycoprotein concentrations are 0.828 mg/ml and 0.352 mg/ml, respectively, based on the determination of the weight fractions of protein cited above. Sedimentation equilibrium absorbance data sets (280 nm) at radial increments of 0.001 cm with 20 repeats were obtained at three different rotor speeds of 8,000, 9000, and 12,000 rpm for the trimer construct and 17,000, 19,000, and 21000 rpm for the monomer at a rotor temperature of 4°C. The public domain software program Sedphat 1.8, developed by Peter Schuck, was used for the analysis of the sedimentation equilibrium data to determine molar mass (http://www.analyticalultracentrifugation.com/).

ITC. ITC was carried out using a VP-ITC titration calorimeter system from MicroCal, Inc. The calorimetric cell containing either monomeric or trimeric gp120 was titrated by stepwise additions of D1D2-CD4, and all reactants were dissolved in PBS with 0.35 M NaCl. The concentration of protein in the cell was about 4 μM for monomeric gp120 and 7 to 10 μM for the trimeric proteins. The concentration of D1D2-CD4 in the syringe was about 45 μM in all experiments. All solutions were properly degassed to avoid any formation of bubbles in the calorimeter during stirring. The heat evolved upon each injection of titrant was obtained from the integral of the calorimetric signal. The heat associated with the binding reaction was obtained by subtracting the heat of dilution of D1D2-CD4 from the heat of reaction with the gp120 glycoproteins. Previous structural studies of free CD4 compared to CD4 in complex with gp120 have shown that CD4 does not change conformation. Therefore, most enthalpy detected from gp120-CD4 interaction originates from rearrangements within gp120 (34, 53). The measurements were made at 25°C, 30°C, and 37°C for both the monomeric and trimeric gp120 glycoproteins. The molar concentrations of the proteins were calculated on a binding site basis per molecule as described previously using the following molar extinction coefficients: 74,420 M^{-1} cm^{-1} for gp120, gp120-GCN4, and D457Vgp120-GCN4; 64,650 M^{-1} cm^{-1} for ΔV1V2gp120-GCN4; 63,370 M^{-1} cm^{-1} for ΔV1V2V3gp120-GCN4; and 18,830 M^{-1} cm^{-1} for D1D2-CD4. The values for the enthalpy, affinity, and stoichiometry were obtained by fitting the data to a nonlinear least-squares analysis with Origin software. The enthalpy change (ΔH) is calculated from the difference between the maximal and the minimal kcal/mole of injectant as indicated on the vertical axis of the graphs (see Fig. 5 and 6).

Since we did not know the precise specific activities of the ligands, we used two highly pure, CD4-induced anti-gp120 antibodies, 17b and 48d, to calibrate the activity of the monomeric ΔV1V2gp120 glycoprotein and thereby indirectly calibrate the activity of D1D2-CD4. These human monoclonal antibodies were produced in mouse ascites in SCID mice and purified to homogeneity by protein A affinity chromatography. When the antibodies were run with F105-affinity purified YU2ΔV1V2gp120, we obtained a stoichiometry of approximately 0.9 from each of several two-antibody ITC analysis. Since the antibodies were highly pure, we assumed that their specific activity approached 100%. This allowed us to calibrate the ΔV1V2gp120 proteins at a now-established 90% specific activity and to subsequently determine that the refolded D1D2-CD4 was approximately 80% active by additional ITC.

Detection of sCD4 binding to gp120-GCN4 constructs by sedimentation velocity analysis. Boundary sedimentation velocity analysis was performed with the XLA/I analytical ultracentrifuge at 20°C with rotor speeds of 38,000 and 30,000 for the four-domain CD4 (sCD4) titration of the gp120-GCN4, D457Vgp120-GCN4, and ΔV1V2V3gp120-GCN4 glycoproteins, respectively. Scans were obtained at 280 nm. Sedimentation coefficient distribution analysis was performed as previously described (56), using the public domain software Sedfit developed by Peter Schuck (http://www.analyticalultracentrifugation.com/). The sedimentation boundary velocity data were subjected to maximum entropy regularization (56). This statistical treatment produced distributions consistent with the raw data within 67% confidence limits.

ELISA. An anti-GCN4 monoclonal antibody (MAb) or the anti-C5 sheep antibody D7324 (43) were coated on high protein binding microwell plates (Corning) overnight at 4°C (500 ng/well) in PBS. Wells were then washed once with washing buffer (PBS–0.2% Tween 20 [PBS-T]) and blocked with PBS with 2% nonfat dried milk and 5% fetal bovine serum for 1 h at room temperature (RT). Affinity-purified gp120 proteins were coated for 2 h at RT in PBS-T (200 ng/well). All wells were washed five times in washing buffer. The MAbs (IgGb12, F105, 17b, 39F, and C11) were added to the wells at 2 μg/well and were diluted in 10-fold serial dilutions, followed by incubation for 1 h at RT in washing buffer. After being washed, a secondary antibody anti-human peroxidase conjugate (Sigma) was added to the well at a 1:10,000 dilution in PBS-T and incubated for 1 h at RT. Wells were washed five times, and the enzyme-linked immunosorbent assays (ELISAs) were developed with TMB peroxidase substrate (Bio-Rad) for 15 min at RT. The reaction was stopped with 180 mM HCl, and plates were read at 450 nm.

To assess CD4 binding, the gp120 proteins were coated overnight at 4°C at 200 ng/well in PBS. The next day, the wells were washed once with PBS-T. D1D2-CD4 was added starting at a concentration of 1 μg/well and was serially diluted 10 fold in PBS-T. Following a 2-h incubation at RT, the plates were washed five times with PBS-T. The anti-CD4 monoclonal antibody (Q425) was diluted 1:500 and added to the wells for 1 h at RT in PBS-T containing 1 μM of $CaCl_2$. Plates were washed again five times. Anti-mouse IgG-peroxidase conjugate diluted to 1:10,000 in PBS-T containing 1 μM of $CaCl_2$ was added to the wells for 1 h at RT. Plates were washed five times, and the plates were developed and analyzed as described above.

CCR5 binding assay. Cf2Th/synCCR5 (42) cells were seeded at 3 million cells/well of a six-well plate overnight at 37°C. A total of 200 ng of gp120 (monomer, trimer, and loop-deleted trimer) or a preformed complex of 120/D1D2-CD4 was added to the cells for 1 h at 37°C. The cells were lysed with 1% NP-40, 20 mM Tris (pH 7.4) for 30 min on ice and spun, and the lysate was run on a SDS-PAGE gel. Following transfer to a nitrocellulose membrane, the gp120 was detected with an anti-gp120 rabbit polyclonal serum.

Electron microscopy (EM). The EM analysis of gp120-GCN4 trimers alone and in complex with sCD4 or b12Fab was performed by negative staining EM analysis as previously described (52, 75). Ligand complexes were formed by 30-min RT incubation of the reactants at ~50 μg/ml in borate-buffered saline with a final dilution to ~2.5 μg/ml total protein just prior to use. The molar ratios of the reactants were varied in different preparations to optimize trimer-ligand complex formation. The gp120 trimers or their complexes were affixed to thin carbon membranes, stained with 1% uranyl formate, and mounted on 600-mesh copper grids for analysis. The sample grids were examined and photographed at a nominal magnification of ×100,000 at 100 kV on a Jeol JEM 1200EX EM. The EMs of immune complex images were digitalized on an Agfa (Ridgefield Park, NJ) Duoscan T2500 negative scanner at a scanning resolution of 1,250 pixels per in. Informative particles of gp120 trimer preparations or trimer-ligand complexes were selected, windowed as 256- by 256-pixel images, then centered, and masked.

RESULTS

Production of recombinant gp120 trimeric glycoproteins. We appended the modified trimerization motif GCN4 at the normally cleaved C terminus of gp120 (gp120-GCN4) (Fig. 1A) and, in combination with loop deletions, at two other selected C-terminal sites to enhance crystallization (Fig. 1B). Using plasmids expressing these gp120 variants, we were able to establish stable, inducible *Drosophila* S2 insect lines to produce milligram quantities of monomeric and oligomeric pro-

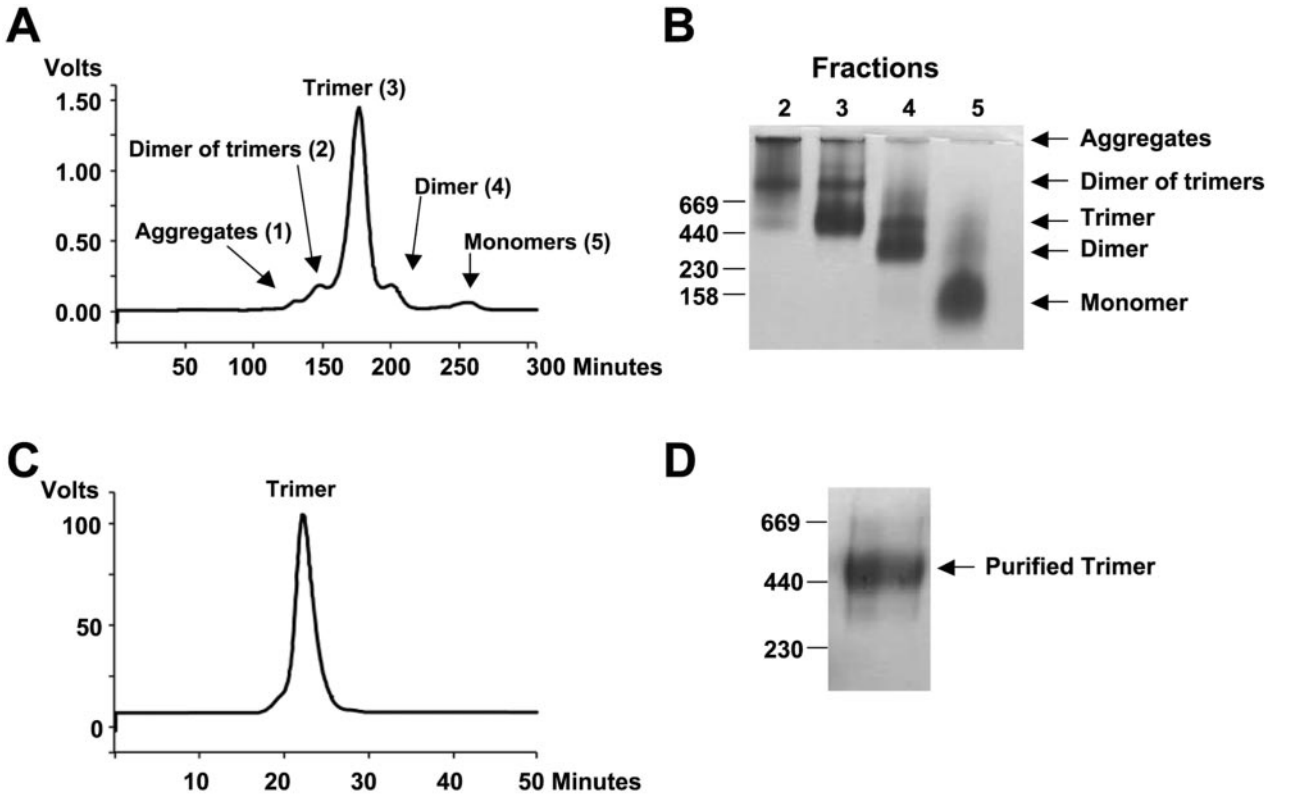

FIG. 2. Gel filtration profile and blue native gels of gp120-GCN4 glycoproteins. (A) Gel filtration profile of the presumptive glycoproteins: aggregates (1), dimer of trimers (2), trimers (3), dimers (4), and monomers (5). (B) Blue native gel. The different fractions are indicated by arrows. Fraction 2, dimer of trimers; fraction 3, trimers; fraction 4, dimers; fraction 5, monomers. (C) Gel filtration profile of purified gp120-GCN4. (D) Blue native gel of the purified gp120-GCN4 trimeric fraction.

teins suitable for biochemical, biophysical, and structural analysis. Since we established high-level production lines for the monomer and oligomeric gp120 variants, we performed most analyses with proteins expressed and purified from these lines. We also produced selected monomeric and trimeric proteins by transient transfection of 293T cells and found few differences between the mammalian cell-produced envelope proteins and the insect-expressed proteins except the expected molecular weight differences due to differential cell-type-associated glycosylation. The set of GCN4-linked proteins were run on SDS-PAGE gels under reducing and nonreducing conditions to assess their homogeneity (Fig. 1B). Under reducing conditions, the GCN4-stabilized molecules migrated in the gel similarly to their monomeric equivalent. Under nonreducing conditions, we always observed a spacing pattern of the GCN4-stabilized proteins that was consistent with oligomerization forms of monomers, dimers, and trimers. The soluble gp120 molecules were predominantly monomers with a minor fraction of dimers determined here by nonreduced SDS-PAGE, as was documented previously (12).

Size exclusion chromatography and blue native gel analysis of the gp120-GCN4 oligomeric molecules. The insect-produced proteins were subjected to size exclusion chromatography under native conditions, which allowed separation of the different oligomeric states (Fig. 2A). By this analysis, the recombinant gp120-GCN4 proteins formed a major peak that, by previous analysis of GCN4-modified glycoproteins (70, 71) and by subsequent analyses described here, was highly likely to be a trimer. Nearly ~90% of the gp120-GCN4 proteins are what we have designated as the trimer fraction, and the other peaks likely correspond to aggregates, dimer of trimers, dimers, and monomers (Fig. 2A).

Gel filtration elution profiles are largely influenced by the radius of the proteins and sometimes can be used to determine the mass of globular proteins relative to calibration markers. However, because the gp120 proteins are nonglobular, the use of gel filtration can be used to determine the oligomeric state (12, 13, 15) but not to accurately determine molecular size relative to the calibration markers. To better define the oligomeric states of the gp120 proteins by another physical method, we analyzed the purified fractions along with known molecular weight calibration proteins (Amersham Pharmacia) on blue native gels (Fig. 2B). Based on the apparent molecular weight of the monomer and the gel mobility positions relative to the molecular weight marker positions, we made assignments of the oligomeric states (Fig. 2B, fractions 2 to 5). The blue native gel analysis confirmed the presence of a presumptive and predominant trimer fraction that could be resolved from a higher-molecular-weight gp120 form, as well as from the dimeric and monomeric gp120 species (Fig. 2B).

The purified trimer proteins were run on gel filtration (Superdex HR 10/30; Amersham Pharmacia), and a fully resolved, symmetric peak consistent with a trimer was observed. A small portion (<3%) of aggregates or dimer of trimers still remained

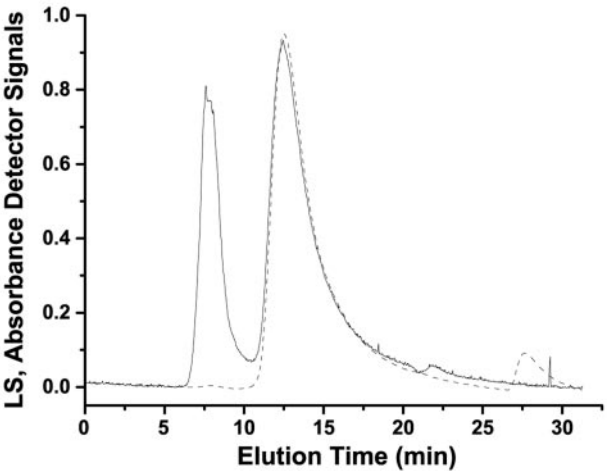

FIG. 3. Size exclusion chromatography with Rayleigh light scattering and absorbance detection of protein peaks. The time elution profile of the presumptive gp120 trimer as detected by light-scattering (solid line) and absorbance (dotted line) measurements is shown. Light-scattering and absorbance detector signals are shown in volts.

(Fig. 2C). The purified trimer was analyzed on blue native gels, migrating as a single species with an apparent molecular mass corresponding to approximately 440 kDa, as determined by comigration with the ferritin marker protein (Fig. 2D). However, apparent molecular mass is likely an overestimate by this method, as similar to gel filtration, nonglobular proteins do not migrate as do the globular molecular weight calibration standards in the blue native gels.

Light scattering, mass spectrometry, and analytical ultracentrifugation molar mass determinations of selected gp120-GCN4 molecules. The gel filtration-purified gp120-GCN4 full-length proteins were used for these experiments. We initially performed a primarily qualitative assessment of the purity of the respective gp120 preparations by SEC-MALS. The SEC-MALS data (light scattering at 90°) for the gp120 trimer preparation is shown in Fig. 3. Overlapping light-scattering (solid line) and absorbance (dashed line) peaks were observed at elution times of 7.8 and 12.5 min, respectively, after correction for volume delay between the detectors. The absorbance signal for the light-scattering peak at 7.8 min was barely detectable, whereas the absorbance of the peak at 12.5 min represented essentially all the protein in the chromatogram. For the monomer preparation, we observed a very low concentration peak at 7.5 min with an overlapping large light-scattering signal comparable to the signal shown in Fig. 3. In addition, we observed a high concentration peak with an overlapping light-scattering signal at 17.2 min (data not shown). The latter peak represents almost all the protein in the chromatogram. The light scattering from a macromolecule was directly proportional to the product of the concentration and the molecular weight. Consequently, we interpret the SEC elution peaks observed in the 7.5- to 7.8-min region to be high-molecular-weight aggregate peaks. Molecular weight analysis using the standard light-scattering equation for isotropically scattering proteins (molar mass, $<5 \times 10^7$) was performed to determine the molar mass of the major peaks for the trimer and monomer preparations (63). The values for the molar mass for both the putative monomer and trimer peaks were within 20% of the anticipated compositional molar mass for each gp120 construct. The SEC-MALS results indicated high purity for the gp120 constructs and correct oligomerization states (respectively, trimer or monomer) with a low level of aggregation.

The sedimentation equilibrium was used to determine the molar mass of the gp120 monomer and gp120-GCN4 trimer constructs. As discussed in Materials and Methods, MALDI-TOF mass spectral analysis of the gp120 monomer gave a molar weight of 83,782. Figure 4A shows the sedimentation equilibrium data for the gp120 monomer construct at 17,000, 19,000, and 21,000 rpm. The global fit for this data gave a molar weight of 85,989. As can be seen in Fig. 4A, bottom, the residuals to the fit were randomly distributed and very close to zero (root mean square deviation [RMSD], 0.01132), indicative of a very good fit. The excellent agreement of sedimentation equilibrium molar mass compared to the mass spectral value supported our analysis of the partial specific volume determinations discussed in Materials and Methods. Using the molar mass of glycosylation obtained from the total MS molar mass value and the protein compositional molar mass of the gp120-GCN4 construct, we calculated a presumptive molar mass for the trimer of 262,725. Figure 4B shows the sedimentation equilibrium data for the gp120 trimer construct at 8,000, 9,000, and 12,000 rpm. The global fit for this data gave a molar weight of 269,482 in excellent agreement with predicted molar weight for the trimer. The residuals of the fit were close to zero (RMSD, 0.01191) but showed small variation from randomness (Fig. 4B, bottom). Large aggregates observed by light scattering are not likely to contribute to the sedimentation equilibrium molar mass measurements, since they would most likely pellet to the bottom of the cell. However, smaller aggregates could form slowly during the time to reach sedimentation equilibrium, and this small amount of aggregation could explain the variation from randomness at the bottom of the centrifuge cell. The sedimentation equilibrium results unequivocally establish that the major and purified oligomeric form of the gp120-GCN4 molecules is virtually all a trimer.

ITC to study selected gp120-GCN4/ligand interactions: thermodynamics and stoichiometry. ITC allows the analysis of the thermodynamic parameters of protein-protein interactions and the determination of the values of enthalpy, entropy, affinity, and stoichiometry of these interactions. Therefore, we sought to examine the thermodynamics of CD4 interaction with the soluble trimers as was done previously for monomeric gp120 (33, 45). Since ITC is often considered the most reliable method available to determine stoichiometry, we were also interested in analyzing the stochiometry of the CD4 interaction with the trimeric proteins. Previously, for two other trimeric lentiviral envelope glycoprotein preparations (simian immunodeficiency virus [SIV] and ADA gp140 glycoproteins), the analysis of CD4 stoichiometry had been examined by different methods and with two contrasting results (29, 73). For novel trimeric proteins possessing three binding sites per oligomer, the demonstration that each binding site within each trimer is functional is difficult and may be complicated by some imprecision in determining the functional activity for each ligand utilized in the ITC analysis (see Materials and Methods).

With those considerations in mind, we first performed microcalorimetry experiments using the affinity- and gel filtra-

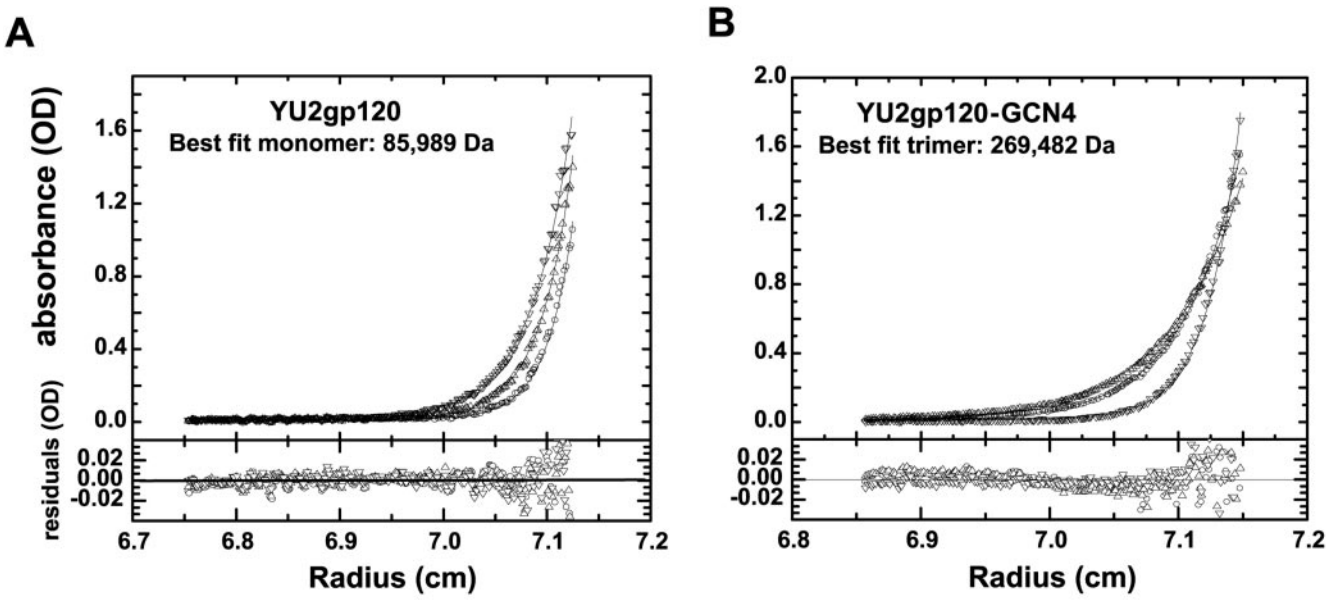

FIG. 4. Sedimentation equilibrium analysis. (A) Sedimentation equilibrium concentration profiles of the gp120 monomer construct obtained at three different rotor speeds: 17,000 rpm (inverted triangles); 19,000 rpm (triangles), and 21,000 rpm (circles). All plots depicted were measured at 280 nm. Solid lines show the best fit to the exponential distributions after nonlinear regression global modeling of the data at the three different rotor speeds. Residuals of the fitted lines to the experimental data are displayed in the lower panel with the corresponding symbols listed above. The best-fit RMSD error is 0.011. (B) Sedimentation equilibrium concentration profiles of the gp120 trimer construct obtained at three different rotor speeds: 8,000 rpm (triangles), 9,000 rpm (circles), and 12,000 rpm (inverted triangles). All plots depicted were measured at 280 nm. Solid lines show the best fit to the exponential distributions after nonlinear regression global modeling of the data at the three different rotor speeds. Residuals of the fitted lines to the experimental data are displayed in the lower panel with the corresponding symbols listed above. The best-fit RMSD error is 0.012.

tion-purified gp120 insect glycoproteins and D1D2-CD4. The binding thermodynamics of D1D2-CD4 to monomeric gp120 was characterized by nanomolar affinity and large enthalpy and entropy values, as reported earlier for four-domain CD4, and had a stoichiometry close to unity (45). The next set of experiments examined the energetics of D1D2-CD4 and the gp120-GCN4 trimer interactions at 37°C (Fig. 5). The enthalpy released upon binding was similar to that observed for the gp120 full-length monomer (−58.7 kcal/mol) (45) and the affinity was 65 nM. Selected ITC experiments were conducted at various temperatures (25°C, 30°C, and 37°C) to obtain the change in heat capacity, ΔCp. (For a summary of the data, see Fig. 7A.) For interaction of the D1D2-CD4 with the gp120-GCN4 trimers, the stoichiometry approached a level of binding two CD4 molecules per trimer (0.65 ± 0.04), indicating that on average, at least two protomers per trimer can bind one CD4 molecule (Fig. 5; see also Fig. 7A). Our interpretation that, on average, two CD4 molecules bind per trimer is supported by the ultracentrifugation analyses (see below).

A set of antibodies that bind to a region of gp120 similar to CD4 are known as the CD4 binding site (CD4BS) antibodies; of the CD4BS antibodies, IgGb12 is the only antibody that can neutralize primary isolates (5, 9). IgGb12 has been previously shown to induce little conformational change upon binding to the gp120 monomer, making it the best ligand for probing the functional activity of each CD4 binding region in a manner independent of large conformational changes (33). To confirm that each binding site within the WT trimeric proteins was fully active, we titrated IgGb12 into the gp120-GCN4 protein solution to perform ITC analysis with this high-affinity, conformationally sensitive ligand. As expected, the affinity of IgGb12 for the gp120-GCN4 trimers was nanomolar and the ΔH value for IgGb12-gp120 interaction was considerably lower than that for CD4 (Fig. 5). Both these parameters were in agreement with previous values for the monomer (33). As seen in Fig. 5, the stoichiometry obtained by ITC was close to 1 (0.85 ± 0.05) (see also Fig. 7B). Therefore, the gp120-GCN4 trimers appear to be at least 85% active, with each protomeric subunit capable of interaction with the conformational IgGb12 ligand. This is in contrast to the more restricted stoichiometry observed that on average only two D1D2-CD4 molecules can bind per trimer. This interpretation is supported by the ultracentrifugation analyses (see below) but is not unequivocal due to the caveats mentioned above.

We analyzed the interaction of the gel filtration-purified ΔV1V2V3gp120-GCN4 trimers with D1D2-CD4 by ITC. The enthalpy of reaction is −51.1 kcal/mol, the affinity is 909 nM, and (unlike the loop-intact trimers) the stoichiometry approached unity. The interaction of ΔV1V2gp120-GCN4 trimers with D1D2-CD4 had an enthalpy change of −62 kcal/mol, an affinity of 14 nM and a stoichiometry that also approached unity.

We then sought to more definitively demonstrate a potentially more-restricted binding of CD4 to the gp120-GCN4 trimers in comparison to IgGb12. We reasoned that perhaps by reducing the affinity of gp120 to CD4 we might better observe any negative cooperation between protomeric subunits within the gp120-GCN4 trimers. Therefore, we generated trimers that

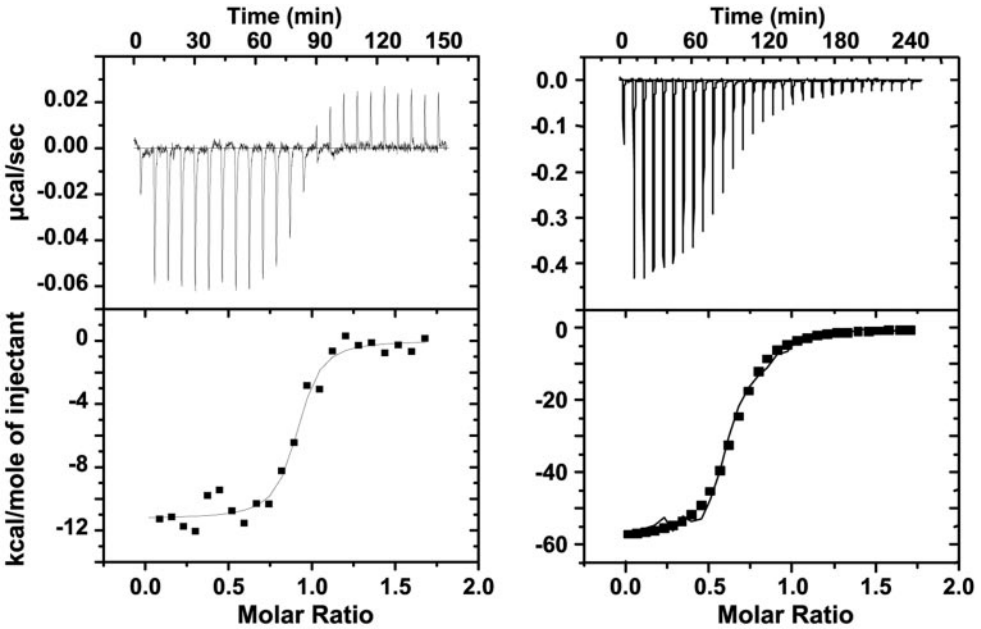

FIG. 5. Isothermal titration calorimetry analyses of the gp120-GCN4 glycoproteins. ITC experiments representing the interactions of YU2gp120-GCN4 with IgGb12 (left) and D1D2-CD4 (right) at 37°C are shown. The top panels represent the raw data as power versus time. The area under each spike is proportional to the heat produced for each injection. The bottom panels represent integrated areas per mole of injected ligand (IgGb12 or D1D2-CD4) as a function of molar ratio. The solid line represents the best nonlinear fit to the experimental data. Enthalpy, $\Delta H = -11.5$ kcal/mol; affinity $K_D = 19$ nM; stoichiometry, $n = 0.88$ (left); enthalpy, $\Delta H = -58.7$ kcal/mol; affinity $K_D = 65$ nM; stoichiometry, $n = 0.64$ (right).

had a decreased affinity for CD4 by introducing a 457 D-to-V change in the CD4 binding site of each gp120 protomer. Changes at residue 457 were previously shown to greatly affect CD4 affinity without completely eliminating IgGb12 binding (50, 60). We determined that the D457V did not affect IgGb12 binding, as shown by ELISA (see Fig. 9). The results obtained from ITC analyses of D1D2-CD4 interacting with the insect-produced, mutant D457Vgp120-GCN4 trimers yielded a strikingly different thermodynamic profile (Fig. 6). As expected the CD4 affinity was greatly reduced (654 nM), and the enthalpy change (ΔH) was −75.6 kcal/mol (on average, per binding event). The enthalpy of binding of D1D2-CD4 to the mutant trimeric gp120 was approximately 20 kcal more favorable than the enthalpy of binding to the WT gp120-GCN4 trimers and to the gp120 monomer (Fig. 7). The stoichiometry of CD4 binding to the D457Vgp120-GCN4 mutant trimer was determined to be 0.24, suggesting a stoichiometry of approximately one D1D2-CD4 molecule bound per trimer. In contrast, the stoichiometry of IgGb12 binding approached unity, indicating that each protomeric CD4 binding region within each trimer was functional (Fig. 6).

We then determined the enthalpy, affinity, and stoichiometry of binding of selected trimers to the CD4-induced antibody 17b (51), which we have determined structurally is able to recognize the same conformation as CD4 (34). We found that for the gp120-GCN4 trimers 17b had an enthalpy of −56.1 kcal/mol, an affinity of 22 nM, and interestingly displayed a restricted stoichiometry of one 17b binding event per trimer ($n = 0.34$). The D457gp120-GCN4 trimers displayed an enthalpy of −32.4 kcal/mol and an affinity of 7 nM and also had a restricted stoichiometry for 17b ($n = 0.23$) at 25°C. In contrast, when the variable V1-V2 loops were removed, the ΔV1V2gp120-GCN4 trimers were able to bind three molecules of 17b per functional trimer, had an affinity of 5 nM, and an enthalpy of −62 kcal/mol. Deletion of the V3 loop greatly reduced 17b affinity and binding, so we did not analyze the ΔV1V2V3gp120-GCN4 molecules in this manner.

Ultracentrifugation of selected gp120-GCN4 molecules with sCD4 to analyze stoichiometry. To further confirm the stoichiometry results obtained by ITC by another method, the binding of sCD4 to the gp120-GCN4, D457Vgp120-GCN4, and ΔV1V2V3gp120-GCN4 constructs was analyzed by boundary sedimentation ultracentrifugation. We determined the velocity changes caused by the formation of respective gp120:CD4 complexes at increasing molar ratios of sCD4. Boundary sedimentation velocity data can be deconvoluted into respective sedimenting species, as outlined in Materials and Methods. Figure 8A shows an overlay of the gp120-GCN4/sCD4 sedimenting complexes formed by the addition of sCD4 at 1:1, 1:2, 1:3, and 1:4 molar excess. The free gp120 trimer has an average weight sedimentation coefficient (s_w) of 8.2S. With the addition of an equal molar concentration of sCD4, a complex is formed with an s_w of 8.62S. Essentially, all the sCD4 is bound, since there is only a small peak at 2.65S, the position of free sCD4. Further additions of two-, three-, and fourfold molar excess sCD4 did not change the sedimentation profile, i.e., all the peaks overlapped with s_w values of 8.98S, 9.02S, and 9.04S, respectively.

Figure 8B shows an overlay of the D457Vgp120-GCN4/sCD4 sedimenting complexes formed by the addition of sCD4 at a 1:1 molar equivalence and 1:3 and 1:5 molar excess. The free gp120 trimer had an s_w of 8.92S. With the addition of

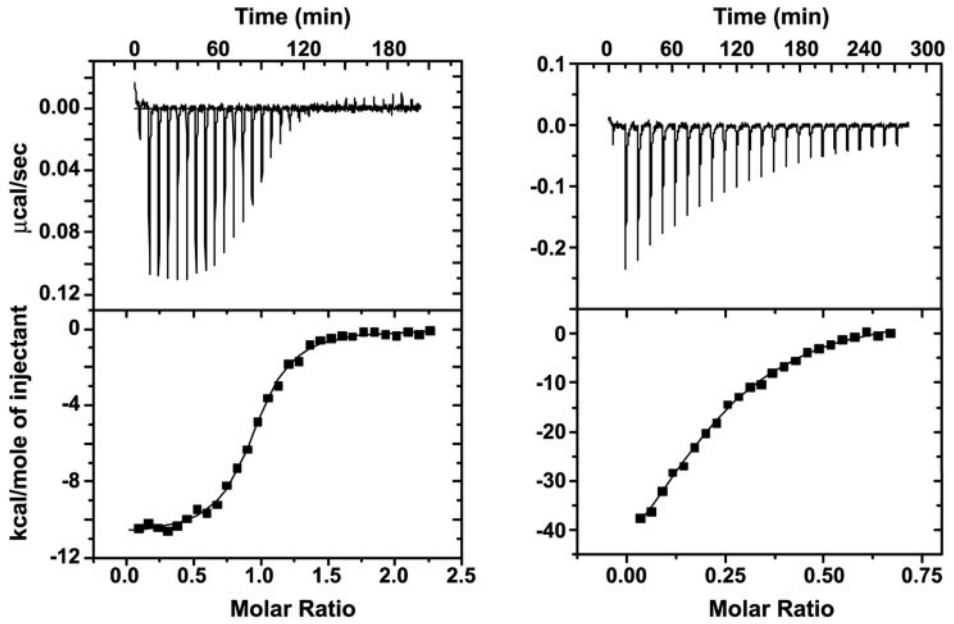

FIG. 6. Isothermal titration calorimetry analyses of the D457Vgp120-GCN4 glycoproteins. ITC experiments representing the interactions of D457Vgp120-GCN4 with IgGb12 (left) and D1D2-CD4 (right) at 37°C are shown. The top panels represent the raw data as power versus time. The area under each spike is proportional to the heat produced for each injection. The bottom panels represent integrated areas per mole of injected ligand (IgGb12 or D1D2-CD4) as a function of molar ratio. The solid line represents the best nonlinear fit to the experimental data. Ethalpy, $\Delta H = -10.7$ kcal/mol; affinity $K_D = 114$ nM; stoichiometry, $n = 0.94$ (left); ethalpy, $\Delta H = -75.6$ kcal/mol; affinity $K_D = 654$ nM; stoichiometry, $n = 0.24$ (right).

equal molar concentration of sCD4, a complex was formed with an s_w of 9.41S. Essentially, all the sCD4 was bound, since there was only a small peak at 2.65S, the position of free sCD4. Further additions of three- and fivefold molar excess sCD4 did not change the sedimentation profile, i.e., all the peaks overlapped with s_w values of 9.50S and 9.53S, respectively.

We interpret these data to mean that for the gp120 trimer, two sCD4 are bound and that for the mutant trimer, one CD4 molecule is bound per trimer. These data also indicate that the WT trimer has a more compact structure than the mutant trimer (i.e., the s_w value is lower for the WT trimer). The overall change in s_w values observed upon addition of sCD4 were smaller than expected, indicating that large conformational rearrangements indeed must occur once CD4 binds to the trimeric molecules.

We also examined the influence of the variable loops on CD4 binding by this method. Figure 8C shows an overlay of the ΔV1V2V3gp120-GCN4/CD4 sedimenting complexes formed by the addition of sCD4 at 1:1, 1:3, and 1:5 molar excess. For the free ΔV1V2V3gp120-GCN4 construct we obtained s_w of 8.40S. Upon the addition of equal molar concentration of sCD4, a complex was formed with an s_w of 8.82S; all the sCD4 was bound, since there was no sedimenting peak in the 2.65S region. The addition of sCD4 at a 1:3 molar ratio to ΔV1V2V3gp120-GCN4 caused a further increase in the s_w value to 9.21S. The addition of sCD4 at a 1:5 molar ratio produced a sedimenting complex that completely overlapped the 1:3 complex. Thus, once the loops are removed from the WT gp120, there appears to be no restriction to the binding of sCD4.

It is also interesting that the loop-deleted construct has an s_w value of 8.40S. The loss of protein mass and glycosylation mass should have reduced the s_w value by between 15 and 20%, yet the s_w value was higher than gp120-GCN4, pointing to the ability of the gp120 protomers to interact, decrease the overall shape of the trimer, and thereby reduce the friction coefficient,

A

CD4-D1D2	Enthalpy (Kcal/mol)	Affinity Kd(nM)	Stoichiometry N	ΔCp (Kcal/K*mol)
YU2 gp 120	- 54.9	36	0.90	-1.8
YU2 gp120-GCN4	- 58.7	65	0.65	-1.8
YU2 D457Vgp120-GCN4	- 75.6	654	0.24	- 4.4
YU2ΔV1V2V3gp120 -GCN4	- 51.1	909	0.86	ND

B

IgGb12	Enthalpy (Kcal/mol)	Affinity Kd(nM)	Stoichiometry N
YU2 gp 120	- 13.0	72	0.80
YU2 gp120-GCN4	- 11.5	19	0.85
YU2 D457Vgp120-GCN4	- 10.7	114	0.94

FIG. 7. Summary table of the thermodynamic values at 37°C. (A) Interactions of selected gp120 glycoproteins with D1D2-CD4. (B) Interactions of selected gp120 glycoproteins with IgGb12.

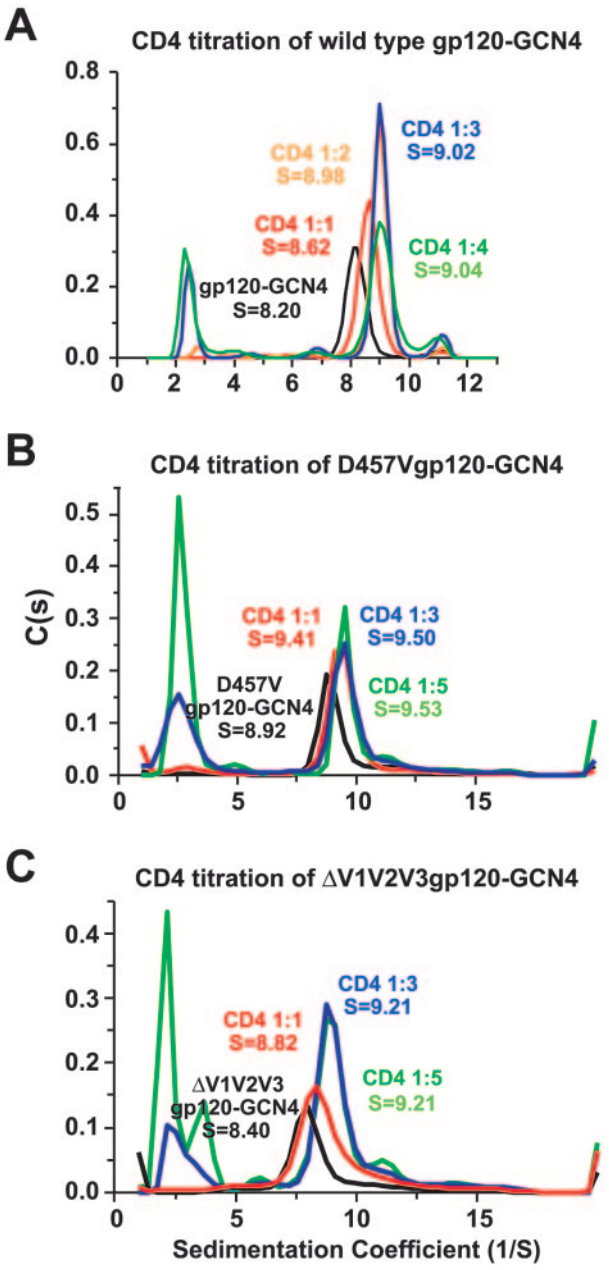

FIG. 8. Sedimentation velocity ultracentrifugation. (A) Overlays of the resolved sedimenting species after the Sedfit software is applied for deconvolution of boundary sedimentation velocity data of free gp120-GCN4 (black), complexes of gp120-GCN4/sCD4 at a 1:1 molar ratio (red), gp120-GCN4/sCD4 at a 1:2 molar ratio (orange), gp120-GCN4/sCD4 at a 1:3 molar ratio (blue), and gp120-GCN4/sCD4 at a 1:4 molar ratio (green). (B) Overlays of the resolved sedimenting species after the Sedfit software is applied for deconvolution of boundary sedimentation velocity data of free D457Vgp120-GCN4 (black), complexes of D457Vgp120-GCN4/sCD4 at a 1:1 molar ratio (red), D457Vgp120-GCN4/sCD4 at a 1:3 molar ratio (blue), and D457Vgp120-GCN4/sCD4 at a 1:5 molar ratio (green). (C) Overlays of the resolved sedimenting species after the Sedfit software is applied for deconvolution of boundary sedimentation velocity data of free ΔV1V2V3gp120-GCN4 (black), complexes of ΔV1V2V3gp120-GCN4/sCD4 at a 1:1 molar ratio (red), ΔV1V2V3gp120-GCN4/sCD4 at a 1:3 molar ratio (blue), and ΔV1V2V3gp120-GCN4/sCD4 at a 1:5 molar ratio (green).

which more than compensates for the s_w reduction due to mass.

Antigenicity of the 120 trimer variants by ELISA with conformational ligands and CCR5 interaction. ELISAs were performed to study the recognition of the recombinant proteins by a small set of well-characterized, conformational, monoclonal antibodies and by sCD4. Both gp120 and gp120-GCN4 and the respective corresponding mutant protein molecules D457Vgp120 and D457Vgp120-GCN4 were recognized by the conformational CD4BS antibodies IgGb12 and F105 (Fig. 9A). In this experiment, the four-domain sCD4 did not bind the D457Vgp120 but retained IgGb12 binding to either the mutant monomer or the trimer. The sCD4 appeared to have a lower affinity and/or stoichiometry for the D457Vgp120-GCN4 trimers than did the WT gp120 monomer and the gp120-GCN4 trimers. These data were in agreement with the ITC analysis that, indeed, both affinity and stoichiometry were affected when the D457V mutation was introduced into gp120 (Fig. 9A). Other gp120 conformational antibodies directed against the V3 loop epitope (39F), a discontinuous epitope in the N and C termini (C11), and the CD4-induced region of gp120 (17b) were also studied. The affinity of 39F to both the WT and mutant trimeric proteins was similar, but the affinity of 17b and C11 to the mutant trimer was lower than to the WT trimer (data not shown).

The gp120-GCN4 insect proteins efficiently bound the CCR5-positive cells in presence of D1D2-CD4, as assessed by Western blotting (Fig. 9B). The binding was inhibited by coincubation of gp120-GCN4 and CD4 with the CD4-induced 17b antibody. This antibody was previously shown to inhibit the interaction of gp120-CD4 with CCR5-expressing cells (66). From these data, we conclude that the gp120-GCN4 proteins retain a native conformational structure and can bind to their natural receptors, CD4 and CCR5.

Morphological examination of the gp120-GCN4 trimers by electron microscopy. The gp120-GCN4 trimers were analyzed by electron microscopy. The gp120 trimer fraction contained a heteromorphic array of molecules with a predominance of forms that were consistent with the expected mass of a trimer (Fig. 10), and the variety of conformations adopted by the trimers suggested intersubunit flexibility. The predominant form displayed a reasonably tight association (Fig. 10A). The first three panels in Fig. 10B show trimers in a compact configuration, similar to that seen in the recently described virion-associated SIV Env trimers (74), where obvious propeller-like trilateral symmetry was displayed. However, in general such forms were in the minority. In addition, some trimers appeared to be only loosely tethered to one another, as seen in the last two panels of Fig. 10B. These observations are consistent with those of virion-associated trimers since, by EM, HIV spikes appear generally less well ordered than SIV trimers (71). Also, the appearance of the HIV gp120 trimeric molecules might be influenced by the random manner by which they become associated with the carbon support membrane (Fig. 11). Excluding the most- and least-compact trimers, the typical trimers measured 22.7 ± 2.7 nm in diameter, which is somewhat larger than the dimensions of the SIV virion trimer and the previously described EMs of recombinant soluble gp140 trimers (58). Despite the fact that the gp140 contains more mass than the gp120 trimer, the potential flexibility resulting from the

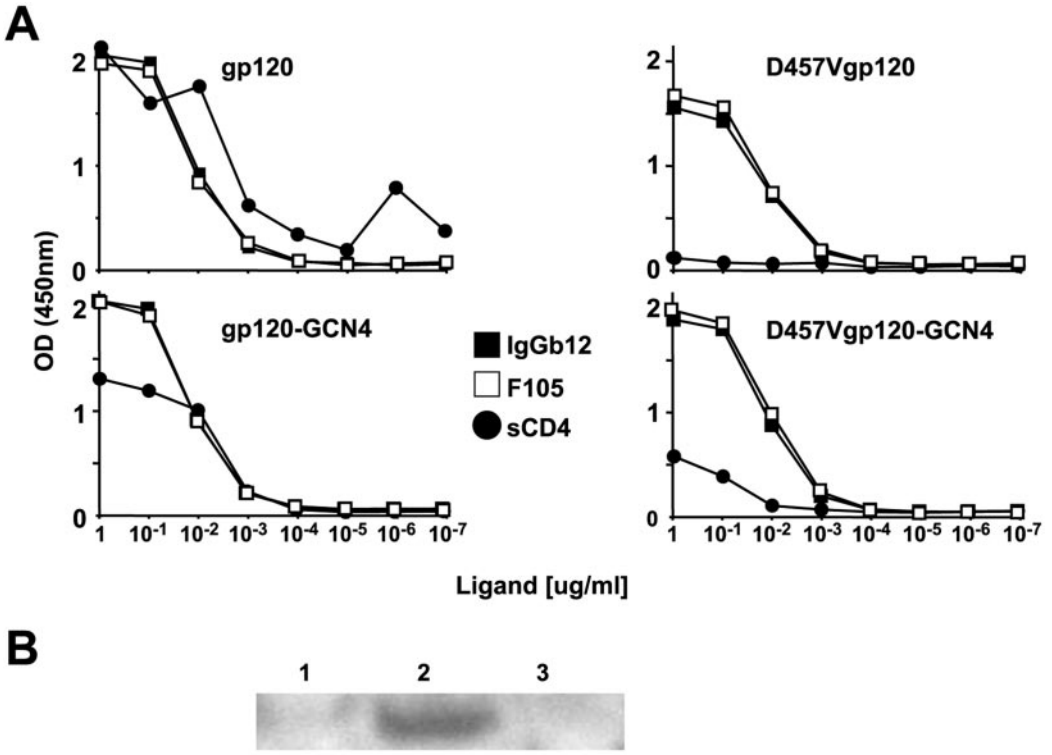

FIG. 9. Antigenicity and functional analysis of the YU2gp120-GCN4 glycoproteins. (A) ELISA analysis of gp120, D457Vgp120, gp120-GCN4, and D457Vgp120-GCN4 derived from YU2 by IgGb12 (closed squares), F105 (open squares), and sCD4 (circles). (B) Western blot analysis of CCR5 binding by gp120-GCN4 (lane 1), gp120-GCN4/D1D2-CD4 (lane 2), and gp120-GCN4/D1D2-CD4/17b (lane 3).

mode of subunit connection might lead to a more open geometry and thus a larger EM profile for the gp120 trimers.

EM analysis of gp120-GCN4-containing complexes showed sCD4 molecules appearing as thin protrusions emanating from one or more of the presumptive gp120 monomeric subunits. Most of the complexes displayed two CD4 molecules bound with the gp120-GCN4 trimers (Fig. 10C, panels 1 to 3). Examples of gp120-GCN4 trimers with one (Fig. 10C, panel 4) and three (Fig. 10C, panel 5) sCD4 bound per trimer are shown. The profile of the CD4 molecule when in complex compared favorably to that previously reported for CD4 plus gp120 or SOS gp140 when bound with 17b (an anti-CD4-induced epitope MAb) (57). We also examined excess IgGb12 binding to gp120-GCN4 (Fig. 10D) and observed images consistent with three, two, or one IgGb12 Fab molecule bound per trimer, with the predominant form appearing to be three IgGb12 Fab fragments per trimer. For both the sCD4- and IgGb12-containing complexes, because of the random nature of the association between the complexes and the carbon support of the EM grid, it was difficult to assign strict ligand stoichiometry.

DISCUSSION

The structural information gained by the atomic-level resolution of the HIV-1 gp120 core glycoprotein was a significant initial step in elucidating the architecture of the HIV-1 Env spike (34) and facilitated molecular modeling of possible trimeric gp120 configurations (35). Since the spike is the major target for neutralizing antibodies and since broadly neutralizing antibodies have yet to be elicited due to the use of imperfect mimics of the native spike, high resolution of the trimeric spike structure may be a necessary step in the design of better Env immunogens. To date, our attempts to produce stable soluble spike mimetics by using heterologous trimerization motifs on the C terminus of HIV-1 gp140 have provided a benefit in immunogenicity over monomeric gp120 (25, 69–72). However, these gp140 trimers have not yet been designed to be amenable to crystallization for various technical reasons such as lack of retention of their native state following deglycosylation. For this reason, we attempted to utilize just the gp120 portion of Env, dispensing with the gp41 ectodomain and appending a heterologous trimerization motif to gp120 in an attempt to mimic gp120 in a form relevant to its trimeric orientation on the native spike. By this approach, we have been able to produce soluble, stable gp120-GCN4 trimers at milligram quantities and at a high level of purity and oligomeric homogeneity, as clearly demonstrated in this study. With these molecules in hand, we sought to perform a thorough characterization of these unique molecules that at the very least represented an advance over most gp140 molecules in their relative oligomeric heterogeneity. The gp120-GCN4 proteins may also provide a means to assess what properties of the Env spike are inherent with gp120 when dissociated from the natural gp41 trimerization domain.

As we have demonstrated here, the gp120-GCN4 molecules (WT and variants) can be efficiently produced in *Drosophila* cells in sufficient quantities to conduct a series of extensive biochemical and biophysical analyses. As shown by size exclu-

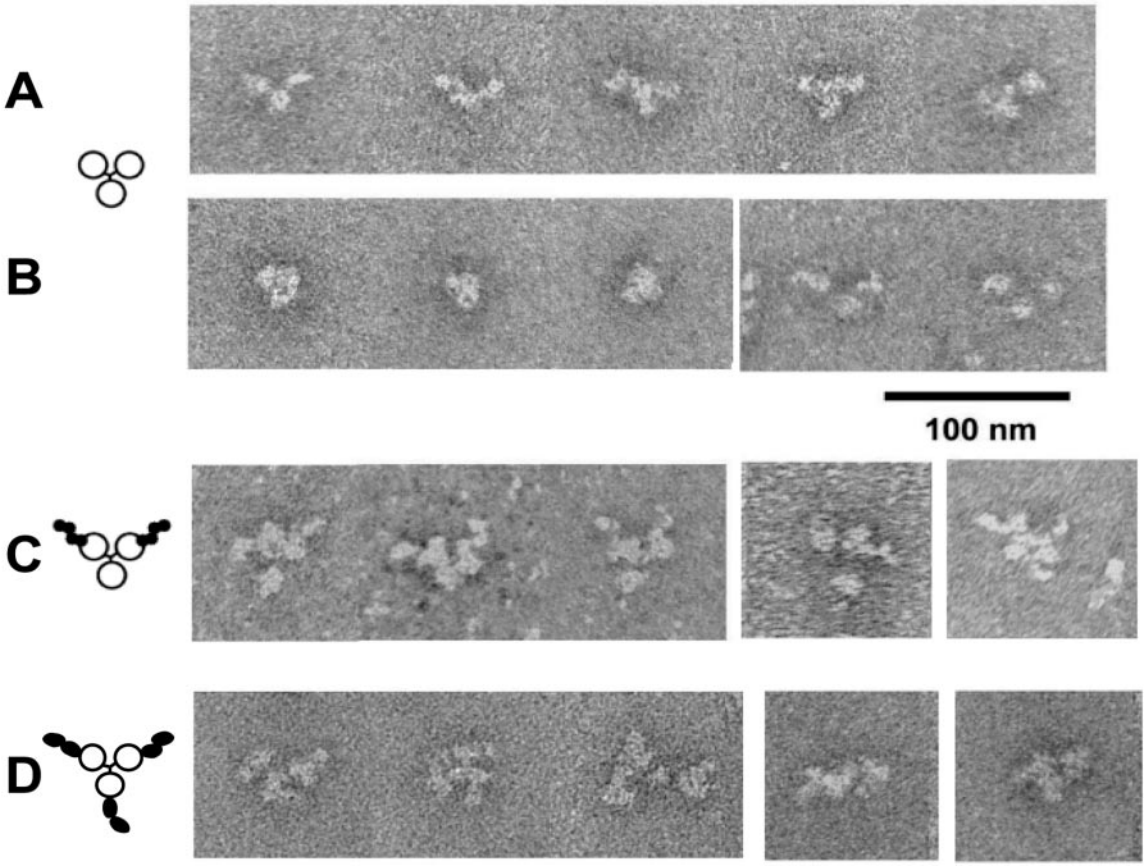

FIG. 10. Electron microscopy and graphic representations of trimeric proteins or complexes protein. Most common forms of gp120-GCN4 (A), other forms of gp120-GCN4 (B), gp120-GCN4/sCD4 complex (C), and gp120-GCN4/b12 Fab complex (D).

sion chromatography, sedimentation equilibrium, and light-scattering analyses, the proteins obtained are homogeneous trimeric molecules, which remained stable following extensive dilution, freeze-thaw, and blue native gel conditions. Identical proteins were also produced from the transient transfection of mammalian cells and allowed us to confirm that the glycan differences of the trimers expressed from the two cell types did not greatly alter their antigenic or thermodynamic properties (not shown).

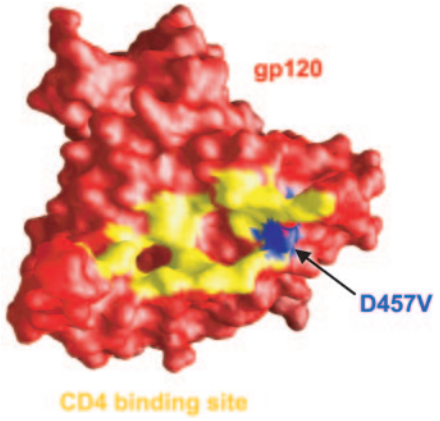

FIG. 11. Molecular surface of the core gp120 molecule with the position of the D457V mutant. The molecular surface of the core gp120 molecule is indicated in red, the binding site of CD4 is shown in yellow, and the mutated residue 457V is shown in blue. The orientation is such that the viral membrane is located toward the top of the page and the cellular membrane is located toward the bottom of the page.

Binding by soluble conformational ligands, as well as their ability to bind CCR5, indicates that the gp120-GCN4 proteins are properly folded within each protomer of the trimer. Microcalorimetric experiments were conducted to study the binding thermodynamics of CD4 to the trimeric molecules and, as with the monomer, large enthalpic and entropic changes occurred following CD4 interaction. By these analyses, there was an indication that on average two CD4 molecules were able to bind to the gp120-GCN4 trimers. This is of interest because a previous study of SIV gp140 trimers demonstrated restricted CD4 binding to these molecules and suggested that this might have physiological relevance (29). In that same study, we noted that the SIV trimers had a lower affinity for CD4 (200 nm) than is normally reported for monomer (1 to 5 nm) and suggested that perhaps this was a manifestation of negative cooperativity of CD4 binding or at the very least that lower affinity was required to observe stoichiometric restriction of CD4 for the Env trimers. So we then asked if lowering the affinity of the gp120-GCN4 trimers for the sCD4 ligand would allow us to better detect a restricted CD4 binding stoichiometry, as ob-

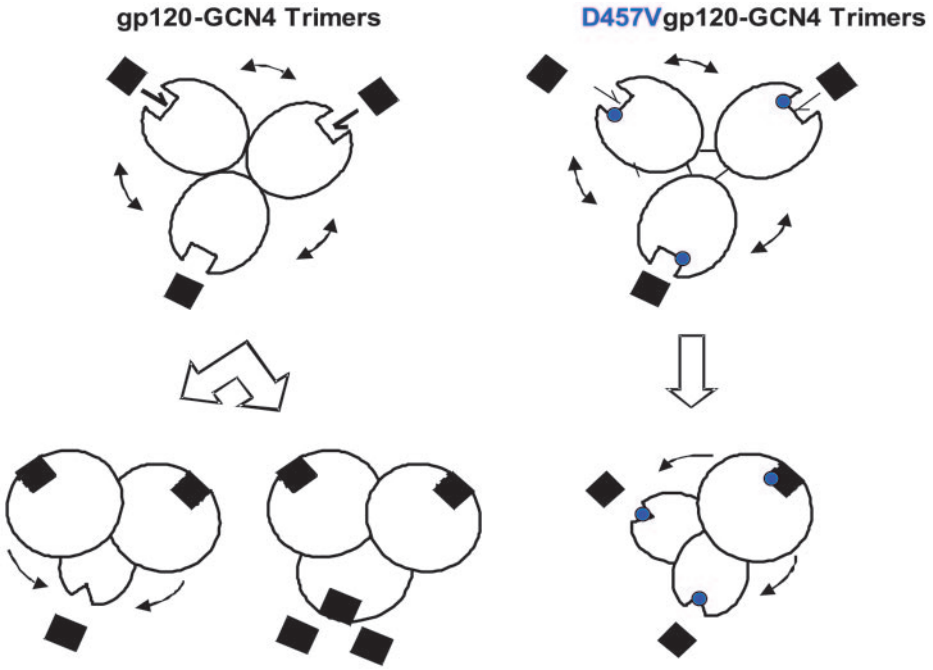

FIG. 12. Model of binding of the CD4 ligand to the YU2gp120-GCN4 variant glycoproteins. Binding of sCD4 to the WT gp120-GCN4 proteins (left) with a restriction of two sCD4 per trimer (with the possible exception that under conditions of vast excess, three sCD4 molecules may bind) and one sCD4 to the mutant D457Vgp120-GCN4 proteins (right). The D457V mutant residue is schematically denoted in blue in the CD4 binding site of the mutant trimers. The relative affinities of CD4 to the two trimer variants are indicated by a thick arrow (WT, high affinity) or a thin arrow (mutant, low affinity). The symbol (■) represents sCD4. The different forms of ovals represent the subunits of the trimeric proteins bound or not bound to sCD4, with the double arrows (top panels) indicating subunit interactions that may oppose the conformational changes associated with ligand binding. Based upon sedimentation analysis, the mutant trimer may be more "open" prior to ligand interaction and is represented in that manner (top right).

served previously for the lower-affinity SIV gp140 trimers (29). We introduced a D-to-V mutation at residue 457, since it was shown previously that mutations to the 457 residue greatly decreased CD4 affinity (with variable effects on IgGb12 recognition) (50, 60).

The mutant obtained in the context of the monomeric protein did not bind sCD4 in this assay but completely retained IgGb12 binding (Fig. 9A). The binding of sCD4 was partially regained in the trimeric context of the D457Vgp120-GCN4 molecules, and we subsequently showed that CD4 recognition was dependent upon the presence of the major variable loops V1/V2 and V3. As noted, the affinity of the mutant trimer for CD4 was reduced (654 nm), and only one CD4 could bind per D457V trimer, which was determined by two independent biophysical methods (ITC and sedimentation velocity) (Fig. 6 and 8). That there might be a more open structure in the D457Vgp120-GCN4 trimers is also reflected in the sedimentation coefficient (s_w) values in comparison to those of the WT (Fig. 8). Within the limits of interpretation, the EM analyses of the gp120-CD4 complexes were generally consistent with the biophysical stoichiometric data.

Interestingly, we could also detect the restricted stoichiometry of one CD4-induced antibody 17b binding to both WT and mutant gp120-GCN4 trimers. Such restricted binding might be a reflection of the lower level of saturable 17b binding to the functional YU2 spike, consistent with the ability of 17b to enhance, but not neutralize, YU2 entry (59). However, when the variable loops V1V2 were removed from WT gp120 trimers, the restricted stoichiometry for 17b binding was no longer apparent. These data are consistent with the observations that V1V2-deleted viruses become more sensitive to neutralization by 17b (11, 31). We know from biophysical studies that 17b and CD4 induce different enthalpy changes (33, 45). However, structural and mutagenic studies indicate that they are able to recognize the same conformation (34, 68); for both these ligands, removal of the variable loops influences the stoichiometry of their binding to the gp120 trimers. Taken together, these data suggest that protomeric interactions occur within the context of the gp120-GCN4 trimers, albeit weak in nature. This interpretation is also consistent with the observation that the sedimentation value of the WT gp120-GCN4 proteins is less than that of V1V2V3-deleted GCN4 proteins, indicating that despite their larger mass, the loop-intact molecules may be more tightly packed (Fig. 8). This suggests considerable flexibility is available in the loop-deleted construct and the ability to accommodate three CD4 molecules.

These data are consistent with a conformational model of the trimeric spike in which the variable loops intimately interact with the variable loops of the adjacent protomer and restrict (mask) conformational rearrangements that are possible in monomeric gp120 (33, 35). IgGb12 does not induce significant rearrangement upon binding to the gp120-GCN4 molecules, the conformational masking does not impact on IgGb12, and, as observed, three molecules of IgGb12 can bind to the gp120-GCN4 trimers. It will be of considerable interest to

determine the mode of IgGb12 binding to native gp120 on virion spikes by EM or other means.

Studies of the structural stability of monomeric gp120 by differential scanning calorimetry have shown that about 250 residues remain unstructured in the native state (36). The large values for the entropy and enthalpy of binding of CD4 to monomeric gp120 first reported by Myszka et al. (45) can be attributed to the structuring of residues, especially those that define the coreceptor site, leading to an increase in binding affinity for the coreceptor. A structure-based thermodynamic approach (39) suggests that 100 to 130 residues are structured upon CD4 binding to monomeric gp120 (36). It is therefore interesting to notice that the enthalpy value is even larger for the binding of one D1D2-CD4 to one mutant D457Vgp120-GCN4 trimer.

Further evidence for a difference in the CD4 binding mechanisms between gp120-GCN4 and D457Vgp120-GCN4 is revealed by the different values obtained for the heat capacity change, ΔCp. ΔCp is proportional to the amount of solvent accessible surface area that is buried upon binding, especially hydrophobic surface (39). Empirical correlations between thermodynamic and structural parameters (39) suggest that the measured ΔC_p of -4.4 kcal/($K\times$ mol) and the measured binding enthalpy are consistent with up to 290 residues buried from the solvent upon binding of one D1D2-CD4 to mutant trimeric D457Vgp120-GCN4, which should be compared to 100 to 130 residues for the binding to monomeric gp120 and WT trimeric gp120-GCN4 (36). We interpret the larger ΔCp values displayed by the lower-affinity mutant as the result of a larger number of residues that become reorganized when one CD4 binds to the mutant trimer, but we do not yet understand why this is associated with lower gp120-CD4 affinity.

Taken together, we interpret these data by the following model (Fig. 12). In the gp120-GCN4 trimers, weak interprotomeric forces exist that oppose the extensive conformational changes induced by the binding of CD4. The binding of two CD4 molecules induces such large conformational changes within the context of the trimer that it is extremely unfavorable for a third binding event to occur. In the context of the mutant, the negative cooperativity is more manifest, presumably due to the larger conformational change induced by CD4 binding to this protein, as indicated by the thermodynamic analysis (the larger ΔH and ΔCp values). We have termed this method low-affinity subunit stoichiometric sensing, and this methodology may have applications for the analysis of other oligomer-ligand interactions. This model might predict that other mutations that lower CD4 affinity may also affect CD4 stoichiometry or that by other methods it might be possible to detect a slower on rate for CD4 onto the WT trimers once two molecules of CD4 were bound. The specific aspects of ligand interactions with trimeric HIV envelope glycoprotein variants continue to be of interest for structural goals and merit further investigation.

This interpretation also raises interesting questions regarding the mechanisms of Env-CD4 interactions in the context of viral entry. As discussed previously for SIV gp140 molecules that also exhibited restricted CD4 binding stoichiometry (29), it is possible that only one or two CD4 binding events per trimer are required to initiate viral entry.

There are properties of these molecules that indicate they are not perfect mimics of the gp120 in the context of the viral spike. For example, they can still bind antibodies that cannot neutralize the YU2 isolate, such as the CD4 binding site antibody F105 and the V3 loop antibody 39F. This is not unexpected, because to fully mimic the properties of the functional Env spike, it may be necessary to precisely constrain the gp120 N and C termini as they exist in association with gp41 in the prefusogenic trimeric viral spike.

We anticipate that if we obtain high-resolution structural information on these molecules, it will aid us in the design of more faithful viral spike mimics that will enhance both immunogenicity and further structural resolution of this viral state. To that end, we are also pursuing high-level resolution structures of these molecules by using selected variant of the trimeric proteins for structural analysis by X-ray crystallography. In fact, we have been able to obtain small crystals from the gel filtration-purified ternary complex D1D2-CD4/17b/ΔV1V2V3Δ497gp120-GCN4 that were grown as previously described (34) under the conditions of 15% 2-propanol, 50 mM Na cacodylate, pH 6.5, and 100 mM trisodium citrate dihydrate. However, we have not yet obtained crystals large enough to analyze their ability to diffract. At the very least, atomic resolution of other molecules would provide valuable information regarding the N and C termini of the gp120 glycoprotein.

ACKNOWLEDGMENTS

We thank Nancy Vieira for doing the mass spectrometry on the gp120 sample and Peter Schuck and Michael Doyle for helpful discussions. The following reagent was obtained through the NIH AIDS Research and Reference Reagent Program, Division of AIDS, NIAID, NIH: soluble human CD4 from Norbert Schulke. We would like to acknowledge Dennis Burton for kindly providing IgGb12 and Edward Berger and the NIH AIDS Research and Reference Reagent Program for providing D1D2-CD4. Thanks to Brenda Hartmann and Toni Garrison for help in the preparation of the figures.

REFERENCES

1. **Adis International Ltd.** 2003. HIV gp120 vaccine - VaxGen: AIDSVAX, AIDSVAX B/B, AIDSVAX B/E, HIV gp120 vaccine - Genentech, HIV gp120 vaccine AIDSVAX - VaxGen, HIV vaccine AIDSVAX - VaxGen. Drugs R D **4:**249–253.
2. **Barnett, S. W., S. Rajasekar, H. Legg, B. Doe, D. H. Fuller, J. R. Haynes, C. M. Walker, and K. S. Steimer.** 1997. Vaccination with HIV-1 gp120 DNA induces immune responses that are boosted by a recombinant gp120 protein subunit. Vaccine **15:**869–873.
3. **Belshe, R. B., G. J. Gorse, M. J. Mulligan, T. G. Evans, M. C. Keefer, J. L. Excler, A. M. Duliege, J. Tartaglia, W. I. Cox, J. McNamara, K. L. Hwang, A. Bradney, D. Montefiori, K. J. Weinhold, et al.** 1998. Induction of immune responses to HIV-1 by canarypox virus (ALVAC) HIV-1 and gp120 SF-2 recombinant vaccines in uninfected volunteers. AIDS **12:**2407–2415.
4. **Berman, P. W., T. J. Gregory, L. Riddle, G. R. Nakamura, M. A. Champe, J. P. Porter, F. M. Wurm, R. D. Hershberg, E. K. Cobb, and J. W. Eichberg.** 1990. Protection of chimpanzees from infection by HIV-1 after vaccination with recombinant glycoprotein gp120 but not gp160. Nature **345:**622–625.
5. **Binley, J. M., T. Wrin, B. Korber, M. B. Zwick, M. Wang, C. Chappey, G. Stiegler, R. Kunert, S. Zolla-Pazner, H. Katinger, C. J. Petropoulos, and D. R. Burton.** 2004. Comprehensive cross-clade neutralization analysis of a panel of anti-human immunodeficiency virus type 1 monoclonal antibodies. J. Virol. **78:**13232–13252.
6. **Bizebard, T., B. Gigant, P. Rigolet, B. Rasmussen, O. Diat, P. Bosecke, S. A. Wharton, J. J. Skehel, and M. Knossow.** 1995. Structure of influenza virus haemagglutinin complexed with a neutralizing antibody. Nature **376:**92–94.
7. **Brighty, D. W., M. Rosenberg, I. S. Chen, and M. Ivey-Hoyle.** 1991. Envelope proteins from clinical isolates of human immunodeficiency virus type 1 that are refractory to neutralization by soluble CD4 possess high affinity for the CD4 receptor. Proc. Natl. Acad. Sci. USA **88:**7802–7805.
8. **Bullough, P. A., F. M. Hughson, J. J. Skehel, and D. C. Wiley.** 1994. Structure of influenza haemagglutinin at the pH of membrane fusion. Nature **371:**37–43.

9. **Burton, D. R., J. Pyati, R. Koduri, S. J. Sharp, G. B. Thornton, P. W. Parren, L. S. Sawyer, R. M. Hendry, N. Dunlop, P. L. Nara, et al.** 1994. Efficient neutralization of primary isolates of HIV-1 by a recombinant human monoclonal antibody. Science **266:**1024–1027.
10. **Cao, J., L. Bergeron, E. Helseth, M. Thali, H. Repke, and J. Sodroski.** 1993. Effects of amino acid changes in the extracellular domain of the human immunodeficiency virus type 1 gp41 envelope glycoprotein. J. Virol. **67:**2747–2755.
11. **Cao, J., N. Sullivan, E. Desjardin, C. Parolin, J. Robinson, R. Wyatt, and J. Sodroski.** 1997. Replication and neutralization of human immunodeficiency virus type 1 lacking the V1 and V2 variable loops of the gp120 envelope glycoprotein. J. Virol. **71:**9808–9812.
12. **Center, R. J., P. L. Earl, J. Lebowitz, P. Schuck, and B. Moss.** 2000. The human immunodeficiency virus type 1 gp120 V2 domain mediates gp41-independent intersubunit contacts. J. Virol. **74:**4448–4455.
13. **Center, R. J., R. D. Leapman, J. Lebowitz, L. O. Arthur, P. L. Earl, and B. Moss.** 2002. Oligomeric structure of the human immunodeficiency virus type 1 envelope protein on the virion surface. J. Virol. **76:**7863–7867.
14. **Center, R. J., J. Lebowitz, R. D. Leapman, and B. Moss.** 2004. Promoting trimerization of soluble human immunodeficiency virus type 1 (HIV-1) Env through the use of HIV-1/simian immunodeficiency virus chimeras. J. Virol. **78:**2265–2276.
15. **Center, R. J., P. Schuck, R. D. Leapman, L. O. Arthur, P. L. Earl, B. Moss, and J. Lebowitz.** 2001. Oligomeric structure of virion-associated and soluble forms of the simian immunodeficiency virus envelope protein in the prefusion activated conformation. Proc. Natl. Acad. Sci. USA **98:**14877–14882.
16. **Chan, D. C., D. Fass, J. M. Berger, and P. S. Kim.** 1997. Core structure of gp41 from the HIV envelope glycoprotein. Cell **89:**263–273.
17. **Choe, H., M. Farzan, Y. Sun, N. Sullivan, B. Rollins, P. D. Ponath, L. Wu, C. R. Mackay, G. LaRosa, W. Newman, N. Gerard, C. Gerard, and J. Sodroski.** 1996. The beta-chemokine receptors CCR3 and CCR5 facilitate infection by primary HIV-1 isolates. Cell **85:**1135–1148.
18. **Colman, P. M., and M. C. Lawrence.** 2003. The structural biology of type I viral membrane fusion. Nat. Rev. Mol. Cell Biol. **4:**309–319.
19. **Connor, R. I., B. T. Korber, B. S. Graham, B. H. Hahn, D. D. Ho, B. D. Walker, A. U. Neumann, S. H. Vermund, J. Mestecky, S. Jackson, E. Fenamore, Y. Cao, F. Gao, S. Kalams, K. J. Kunstman, D. McDonald, N. McWilliams, A. Trkola, J. P. Moore, and S. M. Wolinsky.** 1998. Immunological and virological analyses of persons infected by human immunodeficiency virus type 1 while participating in trials of recombinant gp120 subunit vaccines. J. Virol. **72:**1552–1576.
20. **Culp, J. S., H. Johansen, B. Hellmig, J. Beck, T. J. Matthews, A. Delers, and M. Rosenberg.** 1991. Regulated expression allows high level production and secretion of HIV- 1 gp120 envelope glycoprotein in Drosophila Schneider cells. Biotechnology (New York) **9:**173–177.
21. **Dalgleish, A. G., P. C. Beverley, P. R. Clapham, D. H. Crawford, M. F. Greaves, and R. A. Weiss.** 1984. The CD4 (T4) antigen is an essential component of the receptor for the AIDS retrovirus. Nature **312:**763–767.
22. **Deng, H., R. Liu, W. Ellmeier, S. Choe, D. Unutmaz, M. Burkhart, P. Di Marzio, S. Marmon, R. E. Sutton, C. M. Hill, C. B. Davis, S. C. Peiper, T. J. Schall, D. R. Littman, and N. R. Landau.** 1996. Identification of a major co-receptor for primary isolates of HIV-1. Nature **381:**661–666.
23. **Earl, P. L., W. Sugiura, D. C. Montefiori, C. C. Broder, S. A. Lee, C. Wild, J. Lifson, and B. Moss.** 2001. Immunogenicity and protective efficacy of oligomeric human immunodeficiency virus type 1 gp140. J. Virol. **75:**645–653.
24. **Gallo, S. A., C. M. Finnegan, M. Viard, Y. Raviv, A. Dimitrov, S. S. Rawat, A. Puri, S. Durell, and R. Blumenthal.** 2003. The HIV Env-mediated fusion reaction. Biochim. Biophys. Acta **1614:**36–50.
25. **Grundner, C., Y. Li, M. Louder, J. Mascola, X. Yang, J. Sodroski, and R. Wyatt.** 2005. Analysis of the neutralizing antibody response elicited in rabbits by repeated inoculation with trimeric HIV-1 envelope glycoproteins. Virology **331:**33–46.
26. **Harbury, P. B., T. Zhang, P. S. Kim, and T. Alber.** 1993. A switch between two-, three-, and four-stranded coiled coils in GCN4 leucine zipper mutants. Science **262:**1401–1407.
27. **Helseth, E., U. Olshevsky, C. Furman, and J. Sodroski.** 1991. Human immunodeficiency virus type 1 gp120 envelope glycoprotein regions important for association with the gp41 transmembrane glycoprotein. J. Virol. **65:**2119–2123.
28. **Hill, C. P., D. Worthylake, D. P. Bancroft, A. M. Christensen, and W. I. Sundquist.** 1996. Crystal structures of the trimeric human immunodeficiency virus type 1 matrix protein: implications for membrane association and assembly. Proc. Natl. Acad. Sci. USA **93:**3099–3104.
29. **Kim, M., B. Chen, R. E. Hussey, Y. Chishti, D. Montefiori, J. A. Hoxie, O. Byron, G. Campbell, S. C. Harrison, and E. L. Reinherz.** 2001. The stoichiometry of trimeric SIV glycoprotein interaction with CD4 differs from that of anti-envelope antibody Fab fragments. J. Biol. Chem. **276:**42667–42676.
30. **Koch, M., M. Pancera, P. D. Kwong, P. Kolchinsky, C. Grundner, L. Wang, W. A. Hendrickson, J. Sodroski, and R. Wyatt.** 2003. Structure-based, targeted deglycosylation of HIV-1 gp120 and effects on neutralization sensitivity and antibody recognition. Virology **313:**387–400.
31. **Kolchinsky, P., E. Kiprilov, and J. Sodroski.** 2001. Increased neutralization sensitivity of CD4-independent human immunodeficiency virus variants. J. Virol. **75:**2041–2050.
32. **Korber, B., F. Foley, C. Kuiken, S. Pillai, and J. Sodroski.** 1998. Numbering positions in HIV relative to HXBc2, p. iii-102-iii-103. *In* J. Sodroski (ed.), Human retroviruses and AIDS. Los Alamos National Laboratory, Los Alamos, NM.
33. **Kwong, P. D., M. L. Doyle, D. J. Casper, C. Cicala, S. A. Leavitt, S. Majeed, T. D. Steenbeke, M. Venturi, I. Chaiken, M. Fung, H. Katinger, P. W. Parren, J. Robinson, D. Van Ryk, L. Wang, D. R. Burton, E. Freire, R. Wyatt, J. Sodroski, W. A. Hendrickson, and J. Arthos.** 2002. HIV-1 evades antibody-mediated neutralization through conformational masking of receptor-binding sites. Nature **420:**678–682.
34. **Kwong, P. D., R. Wyatt, J. Robinson, R. W. Sweet, J. Sodroski, and W. A. Hendrickson.** 1998. Structure of an HIV gp120 envelope glycoprotein in complex with the CD4 receptor and a neutralizing human antibody. Nature **393:**648–659.
35. **Kwong, P. D., R. Wyatt, Q. J. Sattentau, J. Sodroski, and W. A. Hendrickson.** 2000. Oligomeric modeling and electrostatic analysis of the gp120 envelope glycoprotein of human immunodeficiency virus. J. Virol. **74:**1961–1972.
36. **Leavitt, S. A., A. Schön, J. C. Klein, U. Manjappara, I. M. Chaiken, and E. Freire.** 2004. Interactions of HIV-1 proteins gp120 and Nef with cellular partners define a novel allosteric paradigm. Curr. Protein Pept. Sci. **5:**1–8.
37. **Lebowitz, J., M. S. Lewis, and P. Schuck.** 2002. Modern analytical ultracentrifugation in protein science: a tutorial review. Protein Sci. **11:**2067–2079.
38. **Lewis, M. S., and R. P. Junghans.** 2000. Ultracentrifugal analysis of molecular mass of glycoproteins of unknown or ill-defined carbohydrate composition. Methods Enzymol. **321:**136–149.
39. **Luque, I., and E. Freire.** 1998. Structure-based prediction of binding affinities and molecular design of peptide ligands. Methods Enzymol. **295:**100–127.
40. **Mascola, J. R., S. W. Snyder, O. S. Weislow, S. M. Belay, R. B. Belshe, D. H. Schwartz, M. L. Clements, R. Dolin, B. S. Graham, G. J. Gorse, M. C. Keefer, M. J. McElrath, M. C. Walker, K. F. Wagner, J. G. McNeil, F. E. McCutchan, D. S. Burke, et al.** 1996. Immunization with envelope subunit vaccine products elicits neutralizing antibodies against laboratory-adapted but not primary isolates of human immunodeficiency virus type 1. J. Infect. Dis. **173:**340–348.
41. **McGaughey, G. B., M. Citron, R. C. Danzeisen, R. M. Freidinger, V. M. Garsky, W. M. Hurni, J. G. Joyce, X. Liang, M. Miller, J. Shiver, and M. J. Bogusky.** 2003. HIV-1 vaccine development: constrained peptide immunogens show improved binding to the anti-HIV-1 gp41 MAb. Biochemistry **42:**3214–3223.
42. **Mirzabekov, T., N. Bannert, M. Farzan, W. Hofmann, P. Kolchinsky, L. Wu, R. Wyatt, and J. Sodroski.** 1999. Enhanced expression, native purification, and characterization of CCR5, a principal HIV-1 coreceptor. J. Biol. Chem. **274:**28745–28750.
43. **Moore, J. P., and R. F. Jarrett.** 1988. Sensitive ELISA for the gp120 and gp160 surface glycoproteins of HIV-1. AIDS Res. Hum. Retrovir. **4:**369–379.
44. **Moore, J. P., J. A. McKeating, Y. X. Huang, A. Ashkenazi, and D. D. Ho.** 1992. Virions of primary human immunodeficiency virus type 1 isolates resistant to soluble CD4 (sCD4) neutralization differ in sCD4 binding and glycoprotein gp120 retention from sCD4-sensitive isolates. J. Virol. **66:**235–243.
45. **Myszka, D. G., R. W. Sweet, P. Hensley, M. Brigham-Burke, P. D. Kwong, W. A. Hendrickson, R. Wyatt, J. Sodroski, and M. L. Doyle.** 2000. Energetics of the HIV gp120-CD4 binding reaction. Proc. Natl. Acad. Sci. USA **97:**9026–9031.
46. **O'Shea, E. K., R. Rutkowski, and P. S. Kim.** 1989. Evidence that the leucine zipper is a coiled coil. Science **243:**538–542.
47. **Pennica, D., W. E. Holmes, W. J. Kohr, R. N. Harkins, G. A. Vehar, C. A. Ward, W. F. Bennett, E. Yelverton, P. H. Seeburg, H. L. Heyneker, D. V. Goeddel, and D. Collen.** 1983. Cloning and expression of human tissue-type plasminogen activator cDNA in E. coli. Nature **301:**214–221.
48. **Posner, M. R., L. A. Cavacini, C. L. Emes, J. Power, and R. Byrn.** 1993. Neutralization of HIV-1 by F105, a human monoclonal antibody to the CD4 binding site of gp120. J. Acquir. Immune Defic. Syndr. **6:**7–14.
49. **Purtscher, M., A. Trkola, A. Grassauer, P. M. Schulz, A. Klima, S. Dopper, G. Gruber, A. Buchacher, T. Muster, and H. Katinger.** 1996. Restricted antigenic variability of the epitope recognized by the neutralizing gp41 antibody 2F5. AIDS **10:**587–593.
50. **Roben, P., J. P. Moore, M. Thali, J. Sodroski, C. F. Barbas, 3rd, and D. R. Burton.** 1994. Recognition properties of a panel of human recombinant Fab fragments to the CD4 binding site of gp120 that show differing abilities to neutralize human immunodeficiency virus type 1. J. Virol. **68:**4821–4828.
51. **Robinson, W. E., Jr., T. Kawamura, M. K. Gorny, D. Lake, J. Y. Xu, Y. Matsumoto, T. Sugano, Y. Masuho, W. M. Mitchell, E. Hersh, et al.** 1990. Human monoclonal antibodies to the human immunodeficiency virus type 1 (HIV-1) transmembrane glycoprotein gp41 enhance HIV-1 infection in vitro. Proc. Natl. Acad. Sci. USA **87:**3185–3189.
52. **Roux, K. H.** 1996. Negative-stain immunoelectron-microscopic analysis of small macromolecules of immunologic significance. Methods **10:**247–256.

53. **Ryu, S. E., P. D. Kwong, A. Truneh, T. G. Porter, J. Arthos, M. Rosenberg, X. P. Dai, N. H. Xuong, R. Axel, R. W. Sweet, et al.** 1990. Crystal structure of an HIV-binding recombinant fragment of human CD4. Nature **348:**419–426.
54. **Sanders, R. W., M. Vesanen, N. Schuelke, A. Master, L. Schiffner, R. Kalyanaraman, M. Paluch, B. Berkhout, P. J. Maddon, W. C. Olson, M. Lu, and J. P. Moore.** 2002. Stabilization of the soluble, cleaved, trimeric form of the envelope glycoprotein complex of human immunodeficiency virus type 1. J. Virol. **76:**8875–8889.
55. **Schonning, K., B. Jansson, S. Olofsson, J. O. Nielsen, and J. S. Hansen.** 1996. Resistance to V3-directed neutralization caused by an N-linked oligosaccharide depends on the quaternary structure of the HIV-1 envelope oligomer. Virology **218:**134–140.
56. **Schuck, P.** 2000. Size-distribution analysis of macromolecules by sedimentation velocity ultracentrifugation and lamm equation modeling. Biophys. J. **78:**1606–1619.
57. **Schulke, N., M. S. Vesanen, R. W. Sanders, P. Zhu, M. Lu, D. J. Anselma, A. R. Villa, P. W. Parren, J. M. Binley, K. H. Roux, P. J. Maddon, J. P. Moore, and W. C. Olson.** 2002. Oligomeric and conformational properties of a proteolytically mature, disulfide-stabilized human immunodeficiency virus type 1 gp140 envelope glycoprotein. J. Virol. **76:**7760–7776.
58. **Srivastava, I. K., L. Stamatatos, E. Kan, M. Vajdy, Y. Lian, S. Hilt, L. Martin, C. Vita, P. Zhu, K. H. Roux, L. Vojtech, C. M. D., J. Donnelly, J. B. Ulmer, and S. W. Barnett.** 2003. Purification, characterization, and immunogenicity of a soluble trimeric envelope protein containing a partial deletion of the V2 loop derived from SF162, an R5-tropic human immunodeficiency virus type 1 isolate. J. Virol. **77:**11244–11259.
59. **Sullivan, N., Y. Sun, J. Li, W. Hofmann, and J. Sodroski.** 1995. Replicative function and neutralization sensitivity of envelope glycoproteins from primary and T-cell line-passaged human immunodeficiency virus type 1 isolates. J. Virol. **69:**4413–4422.
60. **Thali, M., C. Furman, D. D. Ho, J. Robinson, S. Tilley, A. Pinter, and J. Sodroski.** 1992. Discontinuous, conserved neutralization epitopes overlapping the CD4-binding region of human immunodeficiency virus type 1 gp120 envelope glycoprotein. J. Virol. **66:**5635–5641.
61. **Weiss, C. D.** 2003. HIV-1 gp41: mediator of fusion and target for inhibition. AIDS Rev. **5:**214–221.
62. **Weissenhorn, W., A. Dessen, S. C. Harrison, J. J. Skehel, and D. C. Wiley.** 1997. Atomic structure of the ectodomain from HIV-1 gp41. Nature **387:**426–430.
63. **Wen, J., A. T., Philo, J. S.** 1996. Size-exclusion chromatography with on-line-scattering, absorbance, and refractive index detectors for studying proteins and their interactions. Anal. Biochem. **240:**155–166.
64. **Wilson, I. A., J. J. Skehel, and D. C. Wiley.** 1981. Structure of the haemagglutinin membrane glycoprotein of influenza virus at 3 A resolution. Nature **289:**366–373.
65. **Wrin, T., T. P. Loh, J. C. Vennari, H. Schuitemaker, and J. H. Nunberg.** 1995. Adaptation to persistent growth in the H9 cell line renders a primary isolate of human immunodeficiency virus type 1 sensitive to neutralization by vaccine sera. J. Virol. **69:**39–48.
66. **Wu, L., N. P. Gerard, R. Wyatt, H. Choe, C. Parolin, N. Ruffing, A. Borsetti, A. A. Cardoso, E. Desjardin, W. Newman, C. Gerard, and J. Sodroski.** 1996. CD4-induced interaction of primary HIV-1 gp120 glycoproteins with the chemokine receptor CCR-5. Nature **384:**179–183.
67. **Wyatt, R., and J. Sodroski.** 1998. The HIV-1 envelope glycoproteins: fusogens, antigens, and immunogens. Science **280:**1884–1888.
68. **Xiang, S. H., P. D. Kwong, R. Gupta, C. D. Rizzuto, D. J. Casper, R. Wyatt, L. Wang, W. A. Hendrickson, M. L. Doyle, and J. Sodroski.** 2002. Mutagenic stabilization and/or disruption of a CD4-bound state reveals distinct conformations of the human immunodeficiency virus type 1 gp120 envelope glycoprotein. J. Virol. **76:**9888–9899.
69. **Yang, X., M. Farzan, R. Wyatt, and J. Sodroski.** 2000. Characterization of stable, soluble trimers containing complete ectodomains of human immunodeficiency virus type 1 envelope glycoproteins. J. Virol. **74:**5716–5725.
70. **Yang, X., L. Florin, M. Farzan, P. Kolchinsky, P. D. Kwong, J. Sodroski, and R. Wyatt.** 2000. Modifications that stabilize human immunodeficiency virus envelope glycoprotein trimers in solution. J. Virol. **74:**4746–4754.
71. **Yang, X., J. Lee, E. M. Mahony, P. D. Kwong, R. Wyatt, and J. Sodroski.** 2002. Highly stable trimers formed by human immunodeficiency virus type 1 envelope glycoproteins fused with the trimeric motif of T4 bacteriophage fibritin. J. Virol. **76:**4634–4642.
72. **Yang, X., R. Wyatt, and J. Sodroski.** 2001. Improved elicitation of neutralizing antibodies against primary human immunodeficiency viruses by soluble stabilized envelope glycoprotein trimers. J. Virol. **75:**1165–1171.
73. **Zhang, C. W., Y. Chishti, R. E. Hussey, and E. L. Reinherz.** 2001. Expression, purification, and characterization of recombinant HIV gp140. The gp41 ectodomain of HIV or simian immunodeficiency virus is sufficient to maintain the retroviral envelope glycoprotein as a trimer. J. Biol. Chem. **276:**39577–39585.
74. **Zhu, P., E. Chertova, J. Bess, Jr., J. D. Lifson, L. O. Arthur, J. Liu, K. A. Taylor, and K. H. Roux.** 2003. Electron tomography analysis of envelope glycoprotein trimers on HIV and simian immunodeficiency virus virions. Proc. Natl. Acad. Sci. USA **100:**15812–15817.
75. **Zhu, P., W. C. Olson, and K. H. Roux.** 2001. Structural flexibility and functional valence of CD4-IgG2 (PRO 542): potential for cross-linking human immunodeficiency virus type 1 envelope spikes. J. Virol. **75:**6682–6686.